
Bayesian Optimization of Multiple Objectives with Different Latencies

Jack M. Buckingham¹ Sebastian Rojas Gonzalez^{2,3} Juergen Branke⁴

Abstract

Multi-objective Bayesian optimization aims to find the Pareto front of optimal trade-offs between a set of expensive objectives while collecting as few samples as possible. In some cases, it is possible to evaluate the objectives separately, and a different latency or evaluation cost can be associated with each objective. This presents an opportunity to learn the Pareto front faster by evaluating the cheaper objectives more frequently. We propose a scalarization based knowledge gradient acquisition function which accounts for the different evaluation costs of the objectives. We prove consistency of the algorithm and show empirically that it significantly outperforms a benchmark algorithm which always evaluates both objectives.

1. Introduction

Bayesian optimization (BO) is a technique for finding the global maximum of an objective function while taking as few samples as possible (Shahriari et al., 2016; Frazier, 2018). Data is collected either sequentially or in batches and a Bayesian model, usually a Gaussian process, is used to estimate both the objective function and the uncertainty in that estimate based on the samples collected so far. An acquisition function is then used to trade-off between exploring regions of the input space with high uncertainty and exploiting regions which are already known to contain good values. In real-world problems, the most common reason for wanting to limit the number of evaluations of the objective function is because it takes a long time to evaluate, but it can also be because evaluating the objective function requires conducting an experiment costing a lot of money.

Furthermore, it is common in real-world problems to have multiple competing objectives. In such problems there is typically no single best solution and instead the aim is to

find a set of optimal trade-offs, where improving on one objective necessarily means regressing in another. This set of optimal trade-offs is referred to as the Pareto front. The use of random scalarizations is a popular technique for solving multi-objective Bayesian optimization problems (Knowles, 2006; Paria et al., 2020). At each step, a randomly chosen scalarization is used to convert the multi-objective problem into a single objective problem. By varying the scalarization throughout the optimization, the different points on the Pareto front are eventually discovered. Instead of using random scalarizations, a more sophisticated approach takes expectation over possible scalarizations, meaning all scalarizations are considered at each step and no time is wasted on scalarizations corresponding to parts of the Pareto front which are already well known (Astudillo & Frazier, 2017).

Traditionally, multi-objective BO assumes that all objectives will be evaluated at each decision vector sampled. However, in practice this might not always make sense. For example, in turbine design, objectives such as efficiency are calculated using a computational fluid dynamics (CFD) simulation while mechanical stresses are calculated using finite element analysis (FEA) (Van den Braembussche, 2008). A similar picture holds in the design of cars where efficiency is measured using CFD while a crashworthiness assessment requires FEA (Liao et al., 2008). In these problems, there are two reasons we may want to evaluate some objectives more often than others. Firstly, some objectives may be cheaper or faster-to-calculate than others and so it may make sense to evaluate those objectives more frequently. Secondly, some objectives may be harder to learn than other objectives, and consequently these objectives require more evaluations for finding the Pareto front. Two features which affect the number of samples required to learn an objective are the characteristic length scale and the level of observation noise.

Problem Statement In this paper, we tackle multi-objective global optimization problems where:

1. objectives can be evaluated separately;
2. all objectives are expensive to some degree;
3. some objectives are harder-to-learn than others.

More formally, let $f^* : \mathcal{X} \rightarrow \mathbb{R}^M$ be an unknown multi-objective function on a space $\mathcal{X} \subset \mathbb{R}^D$, whose components

¹MathSys CDT, University of Warwick, Coventry, UK

²Surrogate Modeling Lab, Gent University, Belgium ³Data Science Institute, Hasselt University, Belgium ⁴Warwick Business School, University of Warwick, Coventry, UK. Correspondence to: Jack Buckingham <jack.buckingham@warwick.ac.uk>.

can be evaluated separately.¹ Suppose we can make observations of f^* according to the model

$$y_m = f_m^*(\mathbf{x}) + \varepsilon_m, \quad \varepsilon_m \sim \mathcal{N}(0, \sigma_m^2) \quad (1)$$

where $m \in \{1, \dots, M\}$ is the component of f^* being evaluated, $\mathbf{x} \in \mathcal{X}$ is the input and ε_m represents observation noise. Suppose further that the costs, c_1, \dots, c_M , of evaluating each objective are constant and known.

The problem is to iteratively choose sample locations $\mathbf{x}_1, \mathbf{x}_2, \dots$ and objectives m_1, m_2, \dots to be evaluated such that the total cost of sampling does not exceed a given budget \mathcal{B} , and the expected regret for a decision maker choosing from the predicted Pareto front approximation is minimized. In this paper we assume the objectives are to be maximized, but the minimization case is analogous.

Related Work The optimization of multiple objectives with different latencies (also referred to as heterogeneous objectives) has received most of its attention from the evolutionary algorithms community (Allmendinger et al., 2015; Chugh et al., 2018; Blank & Deb, 2022; Mamun et al., 2022; Wang et al., 2022). A recent review is given in (Allmendinger & Knowles, 2021). Evolutionary algorithms tend to be very sample greedy compared with BO. Consequently, BO is better suited to problems where the objectives take minutes or hours to evaluate. However, we are only aware of one BO algorithm which exploits objectives that can be evaluated separately.

Loka et al. (2022) directly incorporate evaluation of the cheap objectives into a pair of hypervolume-based acquisition functions for BO. Consequently, they are evaluated many times while the acquisition function is optimized. This is only applicable when the cheap objective is extremely cheap, as is the case for an objective with a known analytical formula.

Another variant on the theme of objectives with different latencies is the single or multi-objective optimization problem where the latency of the objective varies over the input space. In these problems the latency is usually learned alongside the objective function. A common approach is to divide a traditional acquisition function by the predicted latency for that input location (Snoek et al., 2012), although this is known to bias the search towards cheaper objectives. This issue has been overcome in recent work by considering non-myopic acquisition functions (Astudillo et al., 2021; Lee et al., 2021).

Contributions

1. We provide a natural extension of the multi-attribute

¹We will use f^* to denote the unknown, true function and f to denote the Gaussian process model.

knowledge-gradient acquisition function (Astudillo & Frazier, 2017) to the case where objectives are evaluated separately and have known, constant latencies / costs.

2. We present experiments in two classes of bi-objective problems, one where the length scales of the objectives differ and one where the variance of the observation noise differs. Our algorithm greatly outperforms a benchmark algorithm which always evaluates both objectives.
3. We demonstrate the importance of taking expectation over scalarizations instead of using a sequence of random scalarizations.
4. We provide a theoretical guarantee that, given an infinite budget, the algorithm will find the global optimum.

2. Background

Bayesian Optimization In single-objective BO, we aim to find the global maximum of an unknown objective function, $f^* : \mathcal{X} \rightarrow \mathbb{R}$,

$$\mathbf{x}^* = \arg \max_{\mathbf{x} \in \mathcal{X}} f^*(\mathbf{x}). \quad (2)$$

Observations are made sequentially, and an *acquisition function* (or *infill criterion*) is used to rate the quality of a proposed sample location. Common choices include expected improvement (Jones et al., 1998) and knowledge gradient (Frazier et al., 2009; Wu & Frazier, 2016).

BO constructs a Bayesian model, f , called the *surrogate model*, describing our belief about the objective function based on the samples we have observed so far. The most common choice for the prior distribution on f is a *Gaussian process* (GP), $f \sim \mathcal{GP}(\mu, k)$ which is fully characterized by its mean and covariance functions, $\mu : \mathcal{X} \rightarrow \mathbb{R}$ and $k : \mathcal{X} \times \mathcal{X} \rightarrow \mathbb{R}$. The simplest way to extend this to a multi-dimensional output space, \mathbb{R}^M , is to model each output as an independent Gaussian process. The result is a *multi-output Gaussian process* (Álvarez et al., 2012) whose fdd's are now fully characterized by a vector-valued mean function $\boldsymbol{\mu} : \mathcal{X} \rightarrow \mathbb{R}^M$ and matrix-valued covariance function $\mathbf{K} : \mathcal{X} \times \mathcal{X} \rightarrow \mathbb{R}^{M \times M}$. Modelling the outputs independently corresponds to \mathbf{K} taking values among the diagonal matrices.

We thus consider a model $f \sim \mathcal{GP}(\boldsymbol{\mu}, \mathbf{K})$, with observations y_m of the m^{th} output corrupted by Gaussian noise. That is,

$$y_m = f_m(\mathbf{x}) + \varepsilon_m, \quad \varepsilon_m \sim \mathcal{N}(0, \sigma_m^2). \quad (3)$$

The noise, ε_m , added to different samples is assumed to be independent. Therefore, conditioning on a set of observations $\mathbf{Y} = \{y_{n,m_n}\}_{n=1}^N$ (an N -element vector) at locations

$\mathbf{X} = \{\mathbf{x}_n\}_{n=1}^N$, we have

$$\begin{aligned} f|\mathbf{Y} &\sim \mathcal{GP}(\boldsymbol{\mu}_{\text{post}}, \mathbf{K}_{\text{post}}), \\ \boldsymbol{\mu}_{\text{post}}(\mathbf{x}_\bullet) &= \boldsymbol{\mu}_\bullet + \mathbf{K}_{\bullet, \mathbf{X}} \mathbf{K}_{\mathbf{X}\mathbf{X} + \Sigma}^{-1} \bar{\mathbf{Y}}, \\ \mathbf{K}_{\text{post}}(\mathbf{x}_\bullet, \mathbf{x}'_\bullet) &= \mathbf{K}_{\bullet\bullet} - \mathbf{K}_{\bullet, \mathbf{X}} \mathbf{K}_{\mathbf{X}\mathbf{X} + \Sigma}^{-1} \mathbf{K}_{\mathbf{X}\bullet}. \end{aligned} \quad (4)$$

and

$$\begin{aligned} \boldsymbol{\mu}_\bullet &= \boldsymbol{\mu}(\mathbf{x}_\bullet), \\ \bar{\mathbf{Y}} &= \mathbf{Y} - [\mu_{m_1}(\mathbf{x}_1) \quad \dots \quad \mu_{m_N}(\mathbf{x}_N)]^T, \\ \mathbf{K}_{\bullet\bullet} &= \mathbf{K}(\mathbf{x}_\bullet, \mathbf{x}'_\bullet), \\ \mathbf{K}_{\bullet, \mathbf{X}} &= [\mathbf{K}_{:, m_1}(\mathbf{x}_\bullet, \mathbf{x}_1) \quad \dots \quad \mathbf{K}_{:, m_N}(\mathbf{x}_\bullet, \mathbf{x}_N)], \\ \mathbf{K}_{\mathbf{X}\bullet} &= [\mathbf{K}_{:, m_1}(\mathbf{x}'_\bullet, \mathbf{x}_1) \quad \dots \quad \mathbf{K}_{:, m_N}(\mathbf{x}'_\bullet, \mathbf{x}_N)]^T, \\ \mathbf{K}_{\mathbf{X}\mathbf{X} + \Sigma} &= \mathbf{K}_{\mathbf{X}\mathbf{X}} + \text{diag}(\sigma_{m_1}^2, \dots, \sigma_{m_N}^2), \\ \mathbf{K}_{\mathbf{X}\mathbf{X}} &= \begin{bmatrix} k_{m_1, m_1}(\mathbf{x}_1, \mathbf{x}_1) & \dots & k_{m_1, m_N}(\mathbf{x}_1, \mathbf{x}_N) \\ \vdots & \ddots & \vdots \\ k_{m_N, m_1}(\mathbf{x}_N, \mathbf{x}_1) & \dots & k_{m_N, m_N}(\mathbf{x}_N, \mathbf{x}_N) \end{bmatrix}, \end{aligned}$$

where we have written $k_{i,j}$ for the $(i, j)^{\text{th}}$ component of \mathbf{K} . During the optimization, let $\mathbb{E}_N[\cdot]$ denote expectation conditional on the N samples collected so far and write $\mu_N(\cdot) = \mathbb{E}_N[f(\cdot)]$ for the posterior mean function with respect to these samples, with mean and covariance functions given by equation (4).

Knowledge Gradient The principle underlying the knowledge gradient acquisition function is that, once the evaluation budget has been reached, we will recommend the input $\mathbf{x}^* \in \mathcal{X}$ which maximizes the posterior mean of the surrogate model. During the optimization, let $\mathbf{x} \in \mathcal{X}$ denote a potential next sample location, and let $y^{\mathbf{x}}$ be the random variable for the observation we might make at this location under the model (3). Then, the posterior mean at some other location $\mathbf{x}' \in \mathcal{X}$ is $\mu_{N+}(\mathbf{x}'; \mathbf{x}) = \mathbb{E}_N[f(\mathbf{x}')|y^{\mathbf{x}}]$. Subtracting the maximum of the current posterior mean of f and taking expectation over $y^{\mathbf{x}}$ gives the *knowledge gradient*,

$$\alpha_{\text{KG}}(\mathbf{x}) = \mathbb{E}_N \left[\max_{\mathbf{x}' \in \mathcal{X}} \mu_{N+}(\mathbf{x}'; \mathbf{x}) \right] - \max_{\mathbf{x}' \in \mathcal{X}} \mu_N(\mathbf{x}'). \quad (5)$$

The knowledge gradient has two main advantages over more commonly used acquisition functions such as expected improvement. Firstly, it naturally handles noisy problems. Secondly, the solution recommended at the end of the optimization does not need to have been previously evaluated. As we shall see in Section 3, the latter advantage makes knowledge gradient significantly easier to extend to the case of separately evaluated objectives than expected improvement. For a full introduction to BO, we refer the reader to (Shahriari et al., 2016; Frazier, 2018).

Multi-Objective Optimization In a multi-objective optimization problem, we have several competing objectives

and, in general, no single point will simultaneously optimize them all. Instead, a set of optimal trade-offs is sought, where an increase in any one objective must come at the expense of a decrease in another. A point in \mathcal{X} is *non-dominated* (or *Pareto optimal*) if it cannot be improved upon in all objectives; the set of all non-dominated points is called the *Pareto set*, and its image under \mathbf{f}^* is the *Pareto front*.

Let $\mathbf{f}^* : \mathcal{X} \rightarrow \mathbb{R}^M$ be our (unknown) multi-dimensional objective function, where each dimension represents a different objective. A common approach to solving multi-objective problems is to use random scalarizations. A scalarizing function is a function $g(\cdot, \boldsymbol{\lambda}) : \mathbb{R}^M \rightarrow \mathbb{R}$, parameterized by weights $\boldsymbol{\lambda}$, which converts a vector in objective space into a scalar. The simplest example is a linear scalarization,

$$g_{\text{linear}}(\mathbf{f}; \boldsymbol{\lambda}) = \boldsymbol{\lambda} \cdot \mathbf{f}, \quad (6)$$

where the weights $\boldsymbol{\lambda} \in \mathbb{R}^M$ satisfy $\lambda_j \geq 0 \forall j$ and $\sum_{j=1}^M \lambda_j = 1$ (i.e., $\boldsymbol{\lambda}$ is a member of the standard simplex $\Lambda \subset \mathbb{R}^M$). The scalarization weights are changed from iteration to iteration to discover points close to different parts of the Pareto front.

There is a choice between applying the scalarization to the data or to the multi-objective model (Chugh, 2022). In the ParEGO algorithm (Knowles, 2006), which uses Chebyshev scalarizations, the scalarization is applied to the vector-valued observations. The resulting scalar values are then modelled with a GP and a single-objective acquisition function is used to select the next sample location. Chugh (2022) refers to this as a mono-surrogate approach. Conversely, Paria et al. (2020) model each objective separately with a GP and then apply the scalarization to the model. The resulting one-dimensional stochastic process can then be plugged into any single-objective acquisition function. Chugh (2022) calls this the multi-surrogate approach and recommends it over the mono-surrogate approach. This is the approach we will take below.

An alternative to selecting a new random scalarization at each step is to instead take expectation over scalarization weights of an acquisition function applied to the scalarized objective. This approach was taken in (Astudillo & Frazier, 2017) for the knowledge gradient. In formulae,

$$\alpha_{\text{expectation}}(\mathbf{x}) = \mathbb{E}_{\boldsymbol{\lambda} \sim p(\boldsymbol{\lambda})} [\alpha_{\text{random}}(\mathbf{x}; \boldsymbol{\lambda})] \quad (7)$$

where $\alpha_{\text{random}}(\cdot; \boldsymbol{\lambda})$ and $\alpha_{\text{expectation}}$ are the acquisition functions which would be used in the cases of random scalarizations and expectation over scalarizations respectively.

Both when using random scalarizations and expectation over scalarizations, there is a choice to be made for the distribution $p(\boldsymbol{\lambda})$ of $\boldsymbol{\lambda}$. Paria et al. (2020) use this to encode the preferences of the decision maker for learning about different areas of the Pareto front. Here we concentrate

on the case where $p(\boldsymbol{\lambda})$ is a uniform distribution over the standard simplex in \mathbb{R}^M .

3. Cost Weighted Multi-Objective Knowledge Gradient

In this section we introduce a novel acquisition function for performing multi-objective Bayesian optimization when objectives may be evaluated separately and have different associated costs. The algorithm is a natural extension of the multi-attribute knowledge gradient (Astudillo & Frazier, 2017) which uses an expectation over linear scalarizations. Our research shows that taking expectation over scalarizations is of particular benefit when objectives may be evaluated separately, and so we also define a version based on random scalarizations in order to make this comparison.

It is important to justify why we chose knowledge gradient over a computationally less expensive acquisition function such as expected improvement. One reason is that knowledge gradient naturally handles observation noise and in noisy problems there is an incentive to sample the noisier objectives more frequently than the less noisy ones. The main motivation however, is that expected improvement requires comparing a potential evaluation candidate to the previously evaluated solutions. If we have not observed all objectives at each of the previous sample locations then we will not be able to scalarize those observations. Neither can we scalarize the potential next observation of just one objective and certainly then cannot compare the two.

3.1. Sampling Strategy and Acquisition Function

For a given weight vector $\boldsymbol{\lambda} \in \Lambda \subset \mathbb{R}^M$ in the standard simplex, the posterior mean of the scalarized surrogate model after N observations is $\mu_N(\boldsymbol{x}'; \boldsymbol{\lambda}) = \mathbb{E}_N[\boldsymbol{\lambda} \cdot \boldsymbol{f}(\boldsymbol{x}')]$. Analogously to Equation (5), let $\boldsymbol{x} \in \mathcal{X}$ denote a potential next sample location, let $m \in \{1, \dots, M\}$ be a potential next objective and let $y_m^{\boldsymbol{x}} = f_m(\boldsymbol{x}) + \varepsilon_m$ be the random variable for the corresponding potential observation. Then the posterior mean of the scalarized model at some other location $\boldsymbol{x}' \in \mathcal{X}$ is $\mu_{N+}(\boldsymbol{x}'; \boldsymbol{x}, m, \boldsymbol{\lambda}) = \mathbb{E}_N[\boldsymbol{\lambda} \cdot \boldsymbol{f}(\boldsymbol{x}') | y_m^{\boldsymbol{x}}]$. Subtracting the maxima of these two functions and taking expectation over $y_m^{\boldsymbol{x}}$ gives the *multi-objective knowledge gradient*,

$$\alpha_{\text{MOKG}}(\boldsymbol{x}, m; \boldsymbol{\lambda}) = \mathbb{E}_N \left[\max_{\boldsymbol{x}' \in \mathcal{X}} \mu_{N+}(\boldsymbol{x}'; \boldsymbol{x}, m, \boldsymbol{\lambda}) \right] - \max_{\boldsymbol{x}' \in \mathcal{X}} \mu_N(\boldsymbol{x}'; \boldsymbol{\lambda}). \quad (8)$$

This is the result for a single scalarization, $\boldsymbol{\lambda}$. Taking expectation over $\boldsymbol{\lambda} \sim p(\boldsymbol{\lambda})$ gives

$$\bar{\alpha}_{\text{MOKG}}(\boldsymbol{x}, m) = \mathbb{E}_{\boldsymbol{\lambda} \sim p(\boldsymbol{\lambda})} [\alpha_{\text{MOKG}}(\boldsymbol{x}, m; \boldsymbol{\lambda})]. \quad (9)$$

In the context of objectives with different evaluation costs,

for example when one objective takes significantly longer to evaluate than another, we divide the MOKG by the cost to evaluate the proposed objective to give a value-per-unit-cost. This is the approach taken by Snoek et al. (2012) in the single objective case. We obtain our main contribution in this work, the *cost-weighted multi-objective knowledge gradient (C-MOKG)* acquisition function,

$$\alpha_{\text{C-MOKG}}(\boldsymbol{x}, m; \boldsymbol{\lambda}, \boldsymbol{c}) = \frac{1}{c_m} \alpha_{\text{MOKG}}(\boldsymbol{x}, m; \boldsymbol{\lambda}), \quad (10a)$$

$$\bar{\alpha}_{\text{C-MOKG}}(\boldsymbol{x}, m; \boldsymbol{c}) = \frac{1}{c_m} \bar{\alpha}_{\text{MOKG}}(\boldsymbol{x}, m), \quad (10b)$$

where \boldsymbol{c} is a vector of costs associated with each of the M objectives.

3.2. Efficient Calculation and Optimization

We will first present a method for calculating and optimizing C-MOKG in the case of random scalarizations using a discrete approximation. We will then use this method alongside a quasi-Monte-Carlo approximation to calculate and optimize C-MOKG when taking expectation over scalarizations.

Discrete Approximation Early work which introduced the knowledge gradient (Frazier et al., 2008; 2009) focused on discrete search spaces. This has inspired a common computational strategy for knowledge gradient in low input dimensions (Wu & Frazier, 2016; Pearce & Branke, 2017; 2018), where a discrete approximation for the input space, \mathcal{X} , is used in the inner optimization, while retaining the full continuous space for the proposed next sample location.

Concretely, let $\mathcal{X}_{\text{disc}}$ be a finite subset approximating \mathcal{X} . Then

$$\alpha_{\text{MOKG}}(\boldsymbol{x}, m; \boldsymbol{\lambda}) \approx \hat{\alpha}_{\text{MOKG}}(\boldsymbol{x}, m; \boldsymbol{\lambda}) = \mathbb{E}_N \left[\max_{\boldsymbol{x}' \in \mathcal{X}_{\text{disc}}} \mu_{N+}(\boldsymbol{x}'; \boldsymbol{x}, m, \boldsymbol{\lambda}) \right] - \max_{\boldsymbol{x}' \in \mathcal{X}_{\text{disc}}} \mu_N(\boldsymbol{x}'; \boldsymbol{\lambda}). \quad (11)$$

Since expectation commutes with linear operators, we can use Equation (4) to write $\mu_{N+}(\boldsymbol{x}'; \boldsymbol{x}, m, \boldsymbol{\lambda})$ as an affine function of the hypothesized observation $y_m^{\boldsymbol{x}}$,

$$\mu_{N+}(\boldsymbol{x}'; \boldsymbol{x}, m, \boldsymbol{\lambda}) = \boldsymbol{\lambda} \cdot \tilde{\boldsymbol{\mu}}(\boldsymbol{x}') + \boldsymbol{\lambda} \cdot \tilde{\boldsymbol{K}}_{:,m}(\boldsymbol{x}', \boldsymbol{x}) \frac{y_m^{\boldsymbol{x}} - \tilde{\mu}_m(\boldsymbol{x})}{\tilde{k}_{m,m}(\boldsymbol{x}, \boldsymbol{x}) + \sigma_m^2}. \quad (12)$$

Here, $\tilde{\boldsymbol{\mu}}$ and $\tilde{\boldsymbol{K}}$ are the posterior mean and covariance functions of \boldsymbol{f} conditional on the N observations so far. It is therefore possible to efficiently calculate $\hat{\alpha}_{\text{MOKG}}$ over \boldsymbol{x} for fixed m using Algorithm 2 in (Frazier et al., 2009). Furthermore, the resulting analytical expression is deterministic and

its derivatives with respect to the candidate input \mathbf{x} can be found with automatic differentiation. Therefore, we can use a deterministic gradient based optimizer such as multistart L-BFGS-B to find the global maximum.

We can then optimize C-MOKG over both m and \mathbf{x} by optimizing the result for every m and choosing the largest. Indeed, writing $[M] = \{1, \dots, M\}$,

$$\begin{aligned} & \max_{\substack{\mathbf{x} \in \mathcal{X} \\ m \in [M]}} \hat{\alpha}_{\text{C-MOKG}}(\mathbf{x}, m; \boldsymbol{\lambda}, \mathbf{c}) \\ &= \max_{m \in [M]} \frac{1}{c_m} \max_{\mathbf{x} \in \mathcal{X}} \hat{\alpha}_{\text{MOKG}}(\mathbf{x}, m; \boldsymbol{\lambda}). \end{aligned} \quad (13)$$

When optimizing knowledge gradient acquisition functions, it is common to neglect the second term in Equation (11) which is constant with respect to \mathbf{x} . However, it is important that we do not neglect this term when performing the outer maximization in Equation (13), since the factor $1/c_m$ means that it is no longer constant with respect to m .

Quasi-Monte-Carlo The discrete approximation from the previous section is sufficient to optimize C-MOKG in the case of a single scalarization. We can extend this to a way to optimize C-MOKG with expectation over scalarizations using a (quasi-)Monte-Carlo approximation (qMC). Indeed,

$$\bar{\alpha}_{\text{C-MOKG}}(\mathbf{x}, m) \approx \frac{1}{Q} \sum_{j=1}^Q \hat{\alpha}_{\text{C-MOKG}}(\mathbf{x}, m; \boldsymbol{\lambda}^{(j)}). \quad (14)$$

Here $\boldsymbol{\lambda}^{(1)}, \dots, \boldsymbol{\lambda}^{(Q)}$ is a qMC sample of size Q . Each term in the sum can be calculated using the discretization technique from the previous section and the average can be optimized with multistart L-BFGS-B.

3.3. Theoretical Results

Let $\Lambda \subset \mathbb{R}^M$ denote the standard simplex. Our first result establishes that the cost-aware multi-objective knowledge gradient is everywhere non-negative. This is a standard result for knowledge-gradient acquisition functions and is the reason that we do not need to take the positive part inside the expectation as is necessary with expected improvement.

Lemma 3.1. *Both forms of the cost-aware multi-objective knowledge gradient are non-negative. That is, for all $\mathbf{x} \in \mathcal{X}$, $m \in \{1, \dots, M\}$ and all $\boldsymbol{\lambda} \in \Lambda$,*

$$\alpha_{\text{C-MOKG}}(\mathbf{x}, m; \boldsymbol{\lambda}) \geq 0 \quad \text{and} \quad \bar{\alpha}_{\text{C-MOKG}}(\mathbf{x}, m) \geq 0,$$

almost surely.

This is a consequence of the maximum of the expectation of a stochastic process being at most the expectation of the

maximum of that process, and is proved as Lemma A.4 in Appendix A.

Our main theoretical contribution ensures that when choosing samples with C-MOKG using either expectation over scalarizations, or random scalarizations, the scalarized objective values associated with the recommendations of the algorithm will converge to the optimal value. We assume no model mismatch by dropping the distinction between \mathbf{f} and \mathbf{f}^* . In particular, since we are considering \mathbf{f}^* to be a GP here rather than a function, the following result should be interpreted as a statement about all possible \mathbf{f}^* together rather than for any individual sample.

For each $N \in \mathbb{N}_0$ and each preference vector $\boldsymbol{\lambda} \in \Lambda$, let

$$\mathbf{x}_{N, \boldsymbol{\lambda}}^* \in \arg \max_{\mathbf{x} \in \mathcal{X}} \mathbb{E}_N[\boldsymbol{\lambda} \cdot \mathbf{f}(\mathbf{x})] \quad (15)$$

be a random variable which maximizes the posterior mean of the scalarized objective at stage N . Thus, $\boldsymbol{\lambda} \cdot \mathbf{f}(\mathbf{x}_{1, \boldsymbol{\lambda}}^*)$, $\boldsymbol{\lambda} \cdot \mathbf{f}(\mathbf{x}_{2, \boldsymbol{\lambda}}^*)$, \dots is the sequence of (noiseless) scalarized objective values we would obtain if we were to use the recommended point at each stage of the optimization. The following theorem tells us that this sequence converges to the true maximum of the scalarized, hidden objective function, $\boldsymbol{\lambda} \cdot \mathbf{f}$.

Theorem 3.2 (Consistency of C-MOKG). *Define the $\mathbf{x}_{n, \boldsymbol{\lambda}}^*$ as in Equation (15). When using C-MOKG with either random scalarizations, or expectation over scalarizations, we have*

$$\forall \boldsymbol{\lambda} \in \Lambda, \quad \boldsymbol{\lambda} \cdot \mathbf{f}(\mathbf{x}_{N, \boldsymbol{\lambda}}^*) \rightarrow \max_{\mathbf{x} \in \mathcal{X}} \boldsymbol{\lambda} \cdot \mathbf{f}(\mathbf{x}) \quad \text{as } N \rightarrow \infty$$

almost surely and in mean.

The proof of this result is based on the work by Bect et al. (2019). It proceeds by showing that $\alpha_{\text{C-MOKG}}$ converges to zero for every choice of $\boldsymbol{\lambda}$ and uses this to prove that the posterior mean converges to the true objective function (possibly up to a constant). Theorem 3.2 then follows easily. We refer the reader to Appendix A for the proofs of these results.

4. Experiments

As observed in the introduction, the two main reasons for evaluating one objective more frequently than another are because it is relatively cheap, and because it is harder to learn. Thus, the largest improvement is seen when the expensive objectives are easier to learn. The experiments on synthetic bi-objective problems in this section demonstrate this in two cases, where the cheaper objective is made harder-to-learn using a shorter length scale and the presence of observation noise, respectively.

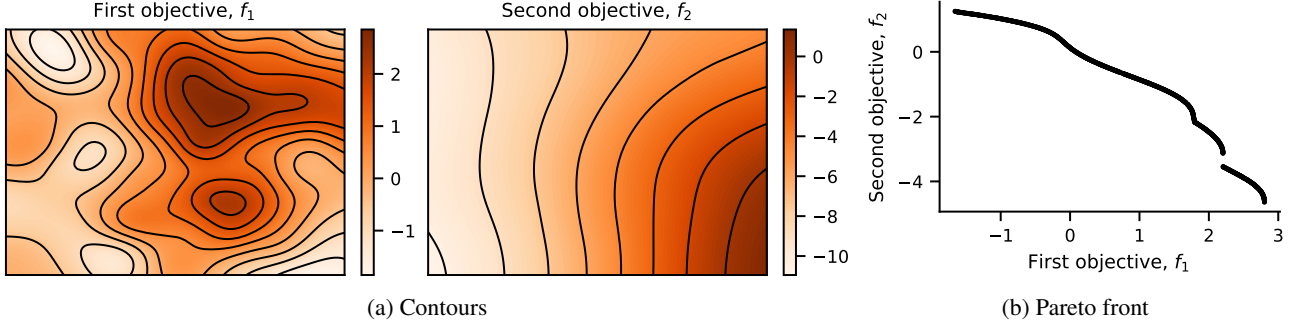


Figure 1. An example from the first set of test problems generated as samples of a GP. Panel (a) shows how the first objective is made harder to learn by giving the GP a shorter length scale. Panel (b) shows the Pareto front of the test problem.

4.1. Synthetic Problems

We test the algorithm on two families of test problems, each with two input dimensions and two objectives. In order to avoid model mismatch, the objectives are generated independently as samples from different Gaussian processes using a Matérn-5/2 kernel.

In the first family of test problems, the first objective has a length scale of 0.2 while the second has a length scale of 1.8. This difference makes the first objective much harder to learn. An example is shown in Figure 1. In this family, no observation noise is added when sampling the problem. In the second family of test problems, both objectives have a length scale of 0.4 and the first is instead made harder to learn by the inclusion of observation noise. The noise added has a standard deviation of 1 which is reasonably large compared with the output scale which is also 1. The second objective is noise free. In both cases, we pretend that the cost or latency of the first objective is 1, while that of the second objective is 10. A full description of the hyper-parameters used to generate these test problems can be found in Appendix B.

4.2. Bayesian Regret Performance Metric

We propose a variant of the often used R2 performance metric for multi-objective optimisation (Hansen & Jaszkiwicz, 1994). This metric assumes a parameterised utility function with a known distribution of the parameter. In our case, we assume $U(\mathbf{x}, \boldsymbol{\lambda}) = \boldsymbol{\lambda} \cdot \mathbf{f}^*(\mathbf{x})$ with $\boldsymbol{\lambda}$ uniformly distributed on the standard simplex. The quality of a solution set S is then the expected utility, i.e.,

$$R2(S) = \mathbb{E}_{\boldsymbol{\lambda} \sim p(\boldsymbol{\lambda})} \left[\max_{\mathbf{x} \in S} \boldsymbol{\lambda} \cdot \mathbf{f}^*(\mathbf{x}) \right]. \quad (16)$$

Our algorithm returns a posterior mean prediction for each objective, \mathbf{f} as an estimate of the true function \mathbf{f}^* . From this, an approximation S of the predicted Pareto front can be derived, e.g., by running a multi-objective evolutionary algorithm on these posterior mean predictions. A decision maker

with a particular utility function defined by $\boldsymbol{\lambda}$ would select a solution $\mathbf{x}_{N,\boldsymbol{\lambda}}^* \in \arg \max_{\mathbf{x} \in S} \mathbb{E}_N[\boldsymbol{\lambda} \cdot \mathbf{f}(\mathbf{x})]$. However, as the resulting Pareto front is based on *predicted* values, the selected solution from this Pareto front doesn't necessarily obtain the utility they hoped for. This can be accounted for by only recording the true utility of the selected solution, $U_N(\boldsymbol{\lambda}) = \boldsymbol{\lambda} \cdot \mathbf{f}^*(\mathbf{x}_{N,\boldsymbol{\lambda}}^*)$. Subtracting this from the maximum possible utility for any solution $\mathbf{x} \in \mathcal{X}$ and taking expectation over $\boldsymbol{\lambda}$ gives the *Bayesian regret*,

$$R_N = \mathbb{E}_{\boldsymbol{\lambda} \sim p(\boldsymbol{\lambda})} \left[\max_{\mathbf{x} \in \mathcal{X}} \boldsymbol{\lambda} \cdot \mathbf{f}^*(\mathbf{x}) - U_N(\boldsymbol{\lambda}) \right]. \quad (17)$$

This is similar to the construction of Bayes regret in (Parija et al., 2020), but allows for a mismatch between the model and true function.

Calculation We calculate the Bayesian regret for each of the 100 repeats. For this, we must find the optimal expected utility $\mathbb{E}_{\boldsymbol{\lambda} \sim p(\boldsymbol{\lambda})}[\max_{\mathbf{x} \in \mathcal{X}} \boldsymbol{\lambda} \cdot \mathbf{f}^*(\mathbf{x})]$. We do this by first estimating 1000 points, $\hat{\mathcal{X}}_{\text{Pareto}}^*$, in the (true) Pareto set using NSGA-II (Deb et al., 2002). Then we average over a quasi-Monte-Carlo sample $(\boldsymbol{\lambda}^{(j)})_{j=1}^{N_\lambda}$ of size $N_\lambda = 1024$, and for each $\boldsymbol{\lambda}^{(j)}$ we restrict the maximization to $\hat{\mathcal{X}}_{\text{Pareto}}^*$,

$$\mathbb{E}_{\boldsymbol{\lambda} \sim p(\boldsymbol{\lambda})} \left[\max_{\mathbf{x} \in \mathcal{X}} \boldsymbol{\lambda} \cdot \mathbf{f}^*(\mathbf{x}) \right] \approx \frac{1}{N_\lambda} \sum_{j=1}^{N_\lambda} \max_{\mathbf{x} \in \hat{\mathcal{X}}_{\text{Pareto}}^*} \boldsymbol{\lambda}^{(j)} \cdot \mathbf{f}^*(\mathbf{x}). \quad (18)$$

We use the same approach to calculate the expected utility,

$$\mathbb{E}_{\boldsymbol{\lambda} \sim p(\boldsymbol{\lambda})} [U_N(\boldsymbol{\lambda})] \approx \frac{1}{N_\lambda} \sum_{j=1}^{N_\lambda} \boldsymbol{\lambda}^{(j)} \cdot \mathbf{f}^*(\mathbf{x}_*^{(j)}), \quad (19)$$

$$\forall j, \quad \mathbf{x}_*^{(j)} \in \arg \max_{\mathbf{x} \in \hat{\mathcal{X}}_{\text{Pareto}}^*} \boldsymbol{\lambda}^{(j)} \cdot \boldsymbol{\mu}_N(\mathbf{x}).$$

Here $\hat{\mathcal{X}}_{\text{Pareto}}^N$ is now an estimate of 1000 points on the Pareto front defined by the posterior mean, $\boldsymbol{\mu}_N$, calculated using NSGA-II. Subtracting Equations (18) and (19) gives an estimate of the Bayesian regret, defined in Equation (17).

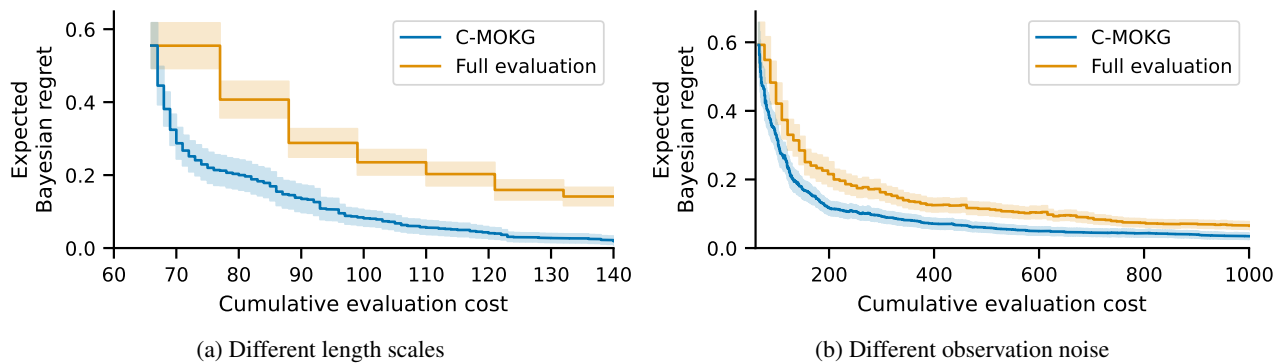


Figure 2. A comparison of the evolution of the expected Bayesian regret between the C-MOKG which evaluates objectives separately (blue), and the benchmark multi-attribute knowledge gradient which always evaluates both objectives. Both algorithms use expectation over scalarizations. For both test problems, C-MOKG outperforms the benchmark because it can save time by skipping samples of the slower, easier-to-learn objective.

4.3. Experimental Details

For each of the two families of test problem, we run the BO 100 times and present the mean of the Bayesian regret. Each repeat uses a different, independently sampled instance of the test problem and a different initial sample of six points generated from a scrambled Sobol’ sequence (Sobol’, 1967). The initial points are all evaluated on both objectives.

We compare our algorithm against a benchmark algorithm which uses the multi-attribute knowledge gradient (Audillo & Frazier, 2017). This always evaluates both objectives but is otherwise identical to our algorithm. For both our acquisition function and the benchmark, we use a uniform 11×11 grid for the discretization $\mathcal{X}_{\text{disc}}$. The expectation over scalarizations is calculated using a quasi-Monte-Carlo estimate using $Q = 16$ points, where each iteration uses the next element from an Q -dimensional scrambled Sobol’ sequence.

For the surrogate model, we use a Matérn-5/2 kernel like the test problem, however, its hyper-parameters are fitted to the observed data using maximum a posteriori estimates. For the first family of test problems, suggestive priors are placed on the length scales to hint to the model that the first objective has a shorter length scale. As observed previously, the algorithm works best when the cheaper objectives are harder to learn. If an engineer knows that an objective is harder to learn then they probably know why. Therefore, using a prior distribution which incorporates this knowledge is natural. Full details of the prior distributions used are included in Appendix B.

4.4. Results

Figure 2 shows the evolution of the expected Bayesian regret over the 100 repeats of the experiment in the two families of test problem. The shaded area shows a 95% confidence

interval in the expected value. In both cases, C-MOKG converges faster. However, the significant levels of noise used in the second family of problems means that convergence is much slower for both algorithms than for the first family.

4.5. Comparison to Random Scalarizations

We have claimed throughout that taking expectation over scalarizations is particularly beneficial when objectives are evaluated separately. In this section, we compare C-MOKG taking expectation over scalarizations, with the version which uses random scalarizations. To generate the random scalarization weights, we use the elements of a scrambled Sobol’ sequence, which ensures that weights are well spread over the simplex.

The results in Figure 3 show a big difference between using expectation over scalarizations (solid) and using random scalarizations (dashed) when objectives are evaluated separately (blue). The difference is not that large when objectives are evaluated together (orange). The reason is probably that some of the random scalarizations will overly favour the slow, easy-to-learn objective. Therefore, the algorithm wastes time taking samples in order to learn about a part of the Pareto front which is already well known. Conversely, the algorithm which takes expectation over scalarizations can look at potential improvement across the whole Pareto front and sample the faster, harder-to-learn objective more often.

4.6. Convergence to the Pareto Front

At every step of the optimization, the algorithm has a prediction of the Pareto front and Pareto set, determined by the posterior mean of the GP surrogate model. To provide intuition on the algorithm, Figure 4 shows this predicted Pareto front (orange) at four points during the optimization

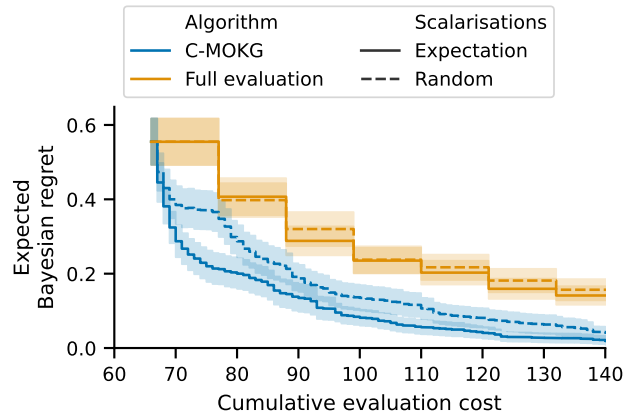


Figure 3. A comparison of the expected Bayesian regret when using random scalarizations (dashed) and expectation over scalarizations (solid), for the first family of test problems. The C-MOKG, which evaluates objectives separately, significantly benefits from using expectation over scalarizations.

in one of the runs for the first family of test problems. The plots also show the image of the predicted Pareto set (blue) which is used to calculate the Bayesian regret metric. We can see that initially the Gaussian process model is a poor surrogate for the true objective function and there is a large discrepancy between the predicted Pareto front and the image of the Pareto set. However, as samples are collected, the model becomes a better representation of the underlying objective function and consequently the predictions of the Pareto front and Pareto set converge on their true values.

5. Conclusion

In this work we have presented a novel acquisition function for performing multi-objective Bayesian optimization when the objectives may be evaluated separately. We have provided a theoretical guarantee for the convergence of the optimization and have experimentally demonstrated its superiority over the natural benchmark.

For future work, we are planning to extend the algorithm also to work with other classes of utility functions such as Chebyshev scalarizations or Cobb-Douglas function. It would also be interesting to extend this work to the case where the latencies must be learned, and to combine our method with those which tackle variation of the latency over the input space (Astudillo et al., 2021; Lee et al., 2021).

Software and Data

The main libraries used were `botorch` (Balandat et al., 2020) and `gpytorch` (Gardner et al., 2018) for the Gaussian processes, and `pygmo` (Biscani & Izzo, 2020) for an implementation of NSGA-II. The implementation of

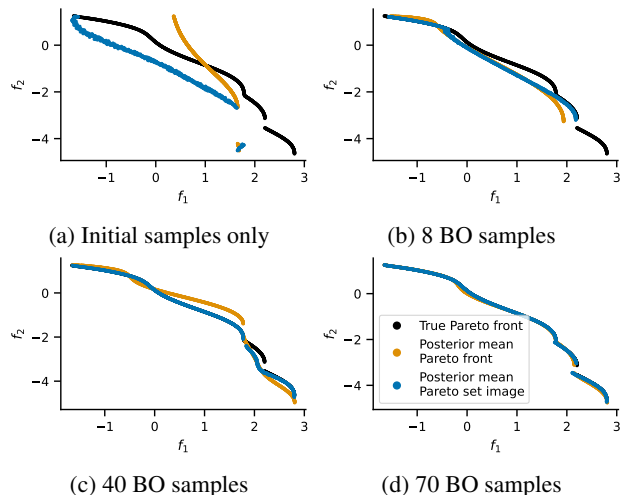


Figure 4. Example of the C-MOKG algorithm converging on the Pareto front in objective space. Shown in orange is the prediction of the Pareto front using the posterior mean of the surrogate model. The image of the predicted Pareto set under the true problem is shown in blue, and represents what outcome the decision maker will get if they choose a point on the predicted Pareto front. The true Pareto front is shown in black. We can see that initially the surrogate model is very poor and so the predicted Pareto front and image of the predicted Pareto set are very different. As more samples are collected with Bayesian optimization (‘BO samples’), both predictions converge on the true Pareto front.

L-BFGS-B used to optimize the acquisition functions and GP hyper-parameters is from `scipy` (Virtanen et al., 2020).

Acknowledgements

The first author was supported by the Engineering and Physical Sciences Research Council through the Mathematics of Systems II Centre for Doctoral Training at the University of Warwick (reference EP/S022244/1). The second author was supported by FWO (Belgium) grant number 1216021N and the Belgian Flanders AI Research Program (VCCM Core Lab).

References

- Allmendinger, R. and Knowles, J. Heterogeneous objectives: State-of-the-art and future research. *arXiv*, art. arXiv:2103.15546, 2 2021.
- Allmendinger, R., Handl, J., and Knowles, J. Multi-objective optimization: When objectives exhibit non-uniform latencies. *European Journal of Operational Research*, 243:497–513, 6 2015. ISSN 03772217. doi: 10.1016/j.ejor.2014.09.033.
- Álvarez, M. A., Rosasco, L., and Lawrence, N. D. Kernels for vector-valued functions: A review. *Foundations and*

- Trends@ in Machine Learning*, 4(3):195–266, 2012. ISSN 1935-8237. doi: 10.1561/22000000036.
- Astudillo, R. and Frazier, P. I. Multi-attribute Bayesian optimization under utility uncertainty. In *NIPS Workshop on Bayesian Optimization*, Long Beach, California, USA, December 2017. URL <https://bayesopt.github.io/papers/2017/41.pdf>.
- Astudillo, R., Jiang, D., Balandat, M., Bakshy, E., and Frazier, P. Multi-step budgeted Bayesian optimization with unknown evaluation costs. *Advances in Neural Information Processing Systems*, 34:20197–20209, 2021.
- Azaïs, J.-M. and Wschebor, M. *Level sets and extrema of random processes and fields*. John Wiley & Sons, 2009. ISBN 978-0-470-40933-6.
- Balandat, M., Karrer, B., Jiang, D., Daulton, S., Letham, B., Wilson, A. G., and Bakshy, E. Botorch: A framework for efficient monte-carlo Bayesian optimization. In Larochelle, H., Ranzato, M., Hadsell, R., Balcan, M., and Lin, H. (eds.), *Advances in Neural Information Processing Systems*, volume 33, pp. 21524–21538. Curran Associates, Inc., 2020. URL <https://proceedings.neurips.cc/paper/2020/file/f5b1b89d98b7286673128a5fb112cb9a-Paper.pdf>.
- Bect, J., Bachoc, F., and Ginsbourger, D. A supermartingale approach to gaussian process based sequential design of experiments. *Bernoulli*, 25, 11 2019. ISSN 1350-7265. doi: 10.3150/18-BEJ1074.
- Biscani, F. and Izzo, D. A parallel global multiobjective framework for optimization: pagmo. *Journal of Open Source Software*, 5(53):2338, 2020. doi: 10.21105/joss.02338.
- Blank, J. and Deb, K. Handling constrained multi-objective optimization problems with heterogeneous evaluation times: proof-of-principle results. *Memetic Computing*, 14:135–150, 6 2022. ISSN 1865-9284. doi: 10.1007/s12293-022-00362-z.
- Chugh, T. Mono-surrogate vs multi-surrogate in multi-objective Bayesian optimisation. In *Proceedings of the Genetic and Evolutionary Computation Conference Companion, GECCO '22*, pp. 2143–2151, New York, NY, USA, 2022. Association for Computing Machinery. ISBN 9781450392686. doi: 10.1145/3520304.3533972.
- Chugh, T., Allmendinger, R., Ojalehto, V., and Miettinen, K. Surrogate-assisted evolutionary biobjective optimization for objectives with non-uniform latencies. In *Proceedings of the Genetic and Evolutionary Computation Conference, GECCO '18*, pp. 609–616, New York, NY, USA, 2018. Association for Computing Machinery. ISBN 9781450356183. doi: 10.1145/3205455.3205514.
- Deb, K., Pratap, A., Agarwal, S., and Meyarivan, T. A fast and elitist multiobjective genetic algorithm: NSGA-II. *IEEE Transactions on Evolutionary Computation*, 6(2): 182–197, 2002. doi: 10.1109/4235.996017.
- Frazier, P. I. Bayesian optimization. In *Recent Advances in Optimization and Modeling of Contemporary Problems*, pp. 255–278. INFORMS, 10 2018. doi: 10.1287/educ.2018.0188.
- Frazier, P. I., Powell, W. B., and Dayanik, S. A knowledge-gradient policy for sequential information collection. *SIAM Journal on Control and Optimization*, 47(5):2410–2439, 2008. doi: 10.1137/070693424.
- Frazier, P. I., Powell, W. B., and Dayanik, S. The knowledge-gradient policy for correlated normal beliefs. *INFORMS Journal on Computing*, 21:599–613, 11 2009. ISSN 1091-9856. doi: 10.1287/ijoc.1080.0314.
- Gardner, J., Pleiss, G., Weinberger, K. Q., Bindel, D., and Wilson, A. G. Gpytorch: Blackbox matrix-matrix gaussian process inference with gpu acceleration. In Bengio, S., Wallach, H., Larochelle, H., Grauman, K., Cesa-Bianchi, N., and Garnett, R. (eds.), *Advances in Neural Information Processing Systems*, volume 31. Curran Associates, Inc., 2018. URL <https://proceedings.neurips.cc/paper/2018/file/27e8e17134dd7083b050476733207ea1-Paper.pdf>.
- Hansen, M. P. and Jaszkievicz, A. Evaluating the quality of approximations to the non-dominated set. Technical report, Institute of Mathematical Modelling, Technical University of Denmark, 1994.
- Jones, D. R., Schonlau, M., and Welch, W. J. Efficient global optimization of expensive black-box functions. *Journal of Global Optimization*, 13:455–492, 12 1998. ISSN 09255001. doi: 10.1023/A:1008306431147.
- Knowles, J. ParEGO: A hybrid algorithm with on-line landscape approximation for expensive multiobjective optimization problems. *IEEE Transactions on Evolutionary Computation*, 10:50–66, 2 2006. ISSN 1089-778X. doi: 10.1109/TEVC.2005.851274.
- Lee, E. H., Eriksson, D., Perrone, V., and Seeger, M. A nonmyopic approach to cost-constrained Bayesian optimization. In de Campos, C. and Maathuis, M. H. (eds.), *Proceedings of the Thirty-Seventh Conference on Uncertainty in Artificial Intelligence*, volume 161 of *Proceedings of Machine Learning Research*, pp. 568–577. PMLR, 27–30 Jul 2021.

- Liao, X., Li, Q., Yang, X., Zhang, W., and Li, W. Multiobjective optimization for crash safety design of vehicles using stepwise regression model. *Structural and Multidisciplinary Optimization*, 35:561–569, 6 2008. ISSN 1615-147X. doi: 10.1007/s00158-007-0163-x.
- Loka, N., Couckuyt, I., Garbuglia, F., Spina, D., Nieuwenhuyse, I. V., and Dhaene, T. Bi-objective Bayesian optimization of engineering problems with cheap and expensive cost functions. *Engineering with Computers*, 1 2022. ISSN 0177-0667. doi: 10.1007/s00366-021-01573-7.
- Mamun, M. M., Singh, H. K., and Ray, T. An approach for computationally expensive multi-objective optimization problems with independently evaluable objectives. *Swarm and Evolutionary Computation*, 75:101146, 12 2022. ISSN 22106502. doi: 10.1016/j.swevo.2022.101146.
- Paria, B., Kandasamy, K., and Póczos, B. A flexible framework for multi-objective Bayesian optimization using random scalarizations. In Adams, R. P. and Gogate, V. (eds.), *Proceedings of The 35th Uncertainty in Artificial Intelligence Conference*, volume 115 of *Proceedings of Machine Learning Research*, pp. 766–776. PMLR, 22–25 Jul 2020. URL <https://proceedings.mlr.press/v115/paria20a.html>.
- Pearce, M. and Branke, J. Bayesian simulation optimization with input uncertainty. In *2017 Winter Simulation Conference (WSC)*, pp. 2268–2278. IEEE, 12 2017. ISBN 978-1-5386-3428-8. doi: 10.1109/WSC.2017.8247958.
- Pearce, M. and Branke, J. Continuous multi-task Bayesian optimisation with correlation. *European Journal of Operational Research*, 270:1074–1085, 11 2018. ISSN 03772217. doi: 10.1016/j.ejor.2018.03.017.
- Pisier, G. *Martingales in Banach Spaces*. Cambridge Studies in Advanced Mathematics. Cambridge University Press, 2016. doi: 10.1017/CBO9781316480588.
- Shahriari, B., Swersky, K., Wang, Z., Adams, R. P., and de Freitas, N. Taking the human out of the loop: A review of Bayesian optimization. *Proceedings of the IEEE*, 104(1):148–175, 2016. doi: 10.1109/JPROC.2015.2494218.
- Snoek, J., Larochelle, H., and Adams, R. P. Practical Bayesian optimization of machine learning algorithms. In Pereira, F., Burges, C., Bottou, L., and Weinberger, K. (eds.), *Advances in Neural Information Processing Systems*, volume 25. Curran Associates, Inc., 2012.
- Sobol’, I. M. On the distribution of points in a cube and the approximate evaluation of integrals. *Zhurnal Vychislitel’noi Matematiki i Matematicheskoi Fiziki*, 7(4): 784–802, 1967.
- Van den Braembussche, R. A. Numerical optimization for advanced turbomachinery design. In Thévenin, D. and Janiga, G. (eds.), *Optimization and Computational Fluid Dynamics*, chapter 6, pp. 147–189. Springer, 2008. ISBN 978-3-540-72152-9. doi: 10.1007/978-3-540-72153-6.
- Virtanen, P., Gommers, R., Oliphant, T. E., Haberland, M., Reddy, T., Cournapeau, D., Burovski, E., Peterson, P., Weckesser, W., Bright, J., van der Walt, S. J., Brett, M., Wilson, J., Millman, K. J., Mayorov, N., Nelson, A. R. J., Jones, E., Kern, R., Larson, E., Carey, C. J., Polat, İ., Feng, Y., Moore, E. W., VanderPlas, J., Laxalde, D., Perktold, J., Cimrman, R., Henriksen, I., Quintero, E. A., Harris, C. R., Archibald, A. M., Ribeiro, A. H., Pedregosa, F., van Mulbregt, P., and SciPy 1.0 Contributors. SciPy 1.0: Fundamental Algorithms for Scientific Computing in Python. *Nature Methods*, 17:261–272, 2020. doi: 10.1038/s41592-019-0686-2.
- Wang, X., Jin, Y., Schmitt, S., and Olhofer, M. Alleviating search bias in Bayesian evolutionary optimization with many heterogeneous objectives. *arXiv*, art. arxiv:2208.12217, 2022. doi: 10.48550/ARXIV.2208.12217.
- Wu, J. and Frazier, P. The parallel knowledge gradient method for batch Bayesian optimization. In Lee, D., Sugiyama, M., Luxburg, U., Guyon, I., and Garnett, R. (eds.), *Advances in Neural Information Processing Systems*, volume 29. Curran Associates, Inc., 2016. URL <https://proceedings.neurips.cc/paper/2016/file/18d10dc6e666eab6de9215ae5b3d54df-Paper.pdf>.

A. Theoretical Results

In this appendix we prove theoretical results associated with the cost-weighted multi-objective knowledge gradient (C-MOKG). The appendix culminates with a proof that, for any scalarization weights, $\boldsymbol{\lambda}$, the estimator of the optimum is asymptotically consistent. The structure of the proof mostly follows that of Bect et al. (2019), without as much of the complex machinery. Unfortunately, we cannot directly apply the results from Bect et al. (2019) because they do not cover the case of random scalarizations.

Since conditional expectations are only defined up to a null event, we qualify the results in this section with ‘almost surely’ (a.s.). The reader should interpret most equalities and inequalities in the proofs of these results to hold almost surely.

A.1. Statistical Model

For the benefit of the reader, we recall the statistical model used. Let $\mathbf{f} \sim \mathcal{GP}(\boldsymbol{\mu}, \mathbf{K})$ be a multi-output Gaussian process with compact index set $\mathcal{X} \subset \mathbb{R}^D$ and defined on a probability space $(\Omega, \mathcal{F}, \mathbb{P})$. here $\boldsymbol{\mu} : \mathcal{X} \rightarrow \mathbb{R}^M$ is the mean function and $\mathbf{K} : \mathcal{X} \times \mathcal{X} \rightarrow \mathbb{R}^{M \times M}$ is the covariance function. We assume that $\boldsymbol{\mu}$ and \mathbf{K} are continuous, and further we use the version of \mathbf{f} with continuous sample paths. Importantly, we do not make a distinction between the GP \mathbf{f} and the ‘true’ function \mathbf{f}^* .

Assume that \mathbf{f} can be observed according to a model

$$y_m = f_m(\mathbf{x}) + \varepsilon_m \quad (20)$$

where $m \in [M] = \{1, \dots, M\}$ indexes the component of \mathbf{f} being evaluated, $\mathbf{x} \in \mathcal{X}$ is the input location and $\varepsilon_m \sim \mathcal{N}(0, \sigma_m^2)$ denotes the observation noise. Let $\mathbf{c} \in (0, \infty)^M$ be a vector of strictly positive evaluation costs associated with each objective. We consider sequentially selected (data-dependent) design points and indices $\mathbf{x}_1, m_1, \mathbf{x}_2, m_2, \dots$ and denote the corresponding observations by $y_{1,m_1}, y_{2,m_2}, \dots$. We write $\varepsilon_{1,m_1}, \varepsilon_{2,m_2}, \dots$ for the independent noise terms added for each observation.

Let $\Lambda = \{\boldsymbol{\lambda} \in [0, \infty)^M : \sum_{j=1}^M \lambda_j = 1\}$ denote the standard simplex in \mathbb{R}^M . We will prove results for both the case of expectation over scalarizations and of random scalarizations. In both cases, we will assume that the probability density $p(\boldsymbol{\lambda})$ is strictly positive everywhere on Λ . For the algorithm which uses random scalarizations, we denote the sequence of scalarization weights by $\boldsymbol{\lambda}_1, \boldsymbol{\lambda}_2, \dots$. For each $n \in \mathbb{N}_0$, denote by $\mathcal{F}_n = \sigma(\{\mathbf{x}_j, m_j, y_{j,m_j}, \varepsilon_{j,m_j}\}_{j=1}^n \cup \{\boldsymbol{\lambda}_j\}_{j=1}^\infty)$, the σ -algebra generated by all the information available at time n along with all the full sequence of scalarization weights. Of course, while harmless, we only need to include the $\boldsymbol{\lambda}_j$ in the case of random scalarizations. In a slight change from the notation in the main text, we then write $\mathbb{E}_n[\cdot]$ for the expectation conditional on \mathcal{F}_n . In order to cleanly handle both algorithms, when a random scalarization weight vector, $\boldsymbol{\lambda}$, is present, we shall consider it part of the conditioned variables,

$$\mathbb{E}_n[\cdot] = \mathbb{E}[\cdot | \sigma(\mathcal{F}_n, \boldsymbol{\lambda})].$$

Then, in order to denote expectation conditional on $\boldsymbol{\lambda}$ alone, we use $\mathbb{E}_{\boldsymbol{\lambda} \sim p(\boldsymbol{\lambda})}[\cdot]$.

Recall our two C-MOKG acquisition functions from the main text. While our definition of \mathbb{E}_n now includes the full sequence of random scalarizations instead of just those up to time n , thanks to the causal structure, this does not change the formulae,

$$\alpha_{\text{C-MOKG}}^n(\mathbf{x}, m; \boldsymbol{\lambda}, \mathbf{c}) = \frac{1}{c_m} \left(\mathbb{E}_n \left[\max_{\mathbf{x}' \in \mathcal{X}} \mu_{n+}^s(\mathbf{x}'; \mathbf{x}, m, \boldsymbol{\lambda}) \right] - \max_{\mathbf{x}' \in \mathcal{X}} \mu_n^s(\mathbf{x}'; \boldsymbol{\lambda}) \right), \quad (21a)$$

$$\bar{\alpha}_{\text{C-MOKG}}^n(\mathbf{x}, m; \mathbf{c}) = \mathbb{E}_{\boldsymbol{\lambda} \sim p(\boldsymbol{\lambda})} [\alpha_{\text{C-MOKG}}^n(\mathbf{x}, m; \boldsymbol{\lambda}, \mathbf{c})], \quad (21b)$$

where $\mu_n^s(\mathbf{x}'; \boldsymbol{\lambda}) = \mathbb{E}_n[\boldsymbol{\lambda} \cdot \mathbf{f}(\mathbf{x}')] = \mathbb{E}_n[\boldsymbol{\lambda} \cdot \mathbf{f}(\mathbf{x}') | y_m^{\mathbf{x}}]$ and $y_m^{\mathbf{x}} = f_m(\mathbf{x}) + \varepsilon_m$ is the hypothesised next observation. Note the superscript s used in this appendix, to distinguish the posterior mean of the scalarized GP from the posterior mean of the unscalarized GP which will be introduced before Proposition A.12.

Informally, we will assume that the design points and indices $\mathbf{x}_1, m_1, \mathbf{x}_2, m_2, \dots$ are chosen to maximize the relevant acquisition function at each step. However, the knowledge gradient is not continuous everywhere so it is not obvious that it attains its maximum. Further, in practice we will never perfectly maximize the acquisition function. For these reasons, we assume that the design points are chosen only to be approximate maximizers of the acquisition functions. That is, we assume that there exists a sequence $\eta = (\eta_n)_{n=0}^\infty$ of small, non-negative real numbers satisfying $\eta_n \rightarrow 0$ as $n \rightarrow \infty$ and

such that one of

$$\forall n \in \mathbb{N}_0, \quad \alpha_{\text{C-MOKG}}^n(\mathbf{x}_{n+1}, m_{n+1}; \boldsymbol{\lambda}_{n+1}, \mathbf{c}) > \sup_{\substack{\mathbf{x} \in \mathcal{X} \\ m \in [M]}} \alpha_{\text{C-MOKG}}^n(\mathbf{x}, m; \boldsymbol{\lambda}_{n+1}, \mathbf{c}) - \eta_n, \quad (22a)$$

$$\forall n \in \mathbb{N}_0, \quad \bar{\alpha}_{\text{C-MOKG}}^n(\mathbf{x}_{n+1}, m_{n+1}; \mathbf{c}) > \sup_{\substack{\mathbf{x} \in \mathcal{X} \\ m \in [M]}} \bar{\alpha}_{\text{C-MOKG}}^n(\mathbf{x}, m; \mathbf{c}) - \eta_n, \quad (22b)$$

depending on whether we are using random scalarizations or expectation over scalarization weights. This is referred to as an η -quasi-SUR sequential design by Bect et al. (Bect et al., 2019)².

A.2. Convergence of $\alpha_{\text{C-MOKG}}^n$ to Zero

Definition A.1. By analogy with Bect et al. (2019), let us set up some notation for the *residual uncertainty* associated with each acquisition function at step $n \in \mathbb{N}_0$,

$$\forall \boldsymbol{\lambda} \in \Lambda, \quad H_n(\boldsymbol{\lambda}) = \mathbb{E}_n \left[\max_{\mathbf{x}' \in \mathcal{X}} \boldsymbol{\lambda} \cdot \mathbf{f}(\mathbf{x}') \right] - \max_{\mathbf{x}' \in \mathcal{X}} \mathbb{E}_n[\boldsymbol{\lambda} \cdot \mathbf{f}(\mathbf{x}')], \quad (23a)$$

$$\bar{H}_n = \mathbb{E}_{\boldsymbol{\lambda} \sim p(\boldsymbol{\lambda})}[H_n(\boldsymbol{\lambda})] \quad (23b)$$

Lemma A.2. *The residual uncertainty in Definition A.1 is well defined. That is,*

$$\forall n \in \mathbb{N}_0 \forall \boldsymbol{\lambda} \in \Lambda, \quad H_n(\boldsymbol{\lambda}) < \infty \quad \text{a.s.} \quad \text{and} \quad \forall n \in \mathbb{N}_0, \quad \bar{H}_n < \infty \quad \text{a.s.}$$

Proof. We will consider the first form first. Let $\boldsymbol{\lambda} \in \Lambda$. Then, since all components of $\boldsymbol{\lambda}$ lie between 0 and 1, we have $|\boldsymbol{\lambda} \cdot \mathbf{f}(\mathbf{x}')| \leq \|\mathbf{f}(\mathbf{x}')\|_1$ for all $\mathbf{x}' \in \mathcal{X}$. Therefore,

$$\begin{aligned} H_n(\boldsymbol{\lambda}) &\leq \mathbb{E}_n \left[\max_{\mathbf{x}' \in \mathcal{X}} |\boldsymbol{\lambda} \cdot \mathbf{f}(\mathbf{x}')| \right] + \max_{\mathbf{x}' \in \mathcal{X}} \mathbb{E}_n |\boldsymbol{\lambda} \cdot \mathbf{f}(\mathbf{x}')| \\ &\leq 2\mathbb{E}_n \left[\max_{\mathbf{x}' \in \mathcal{X}} |\boldsymbol{\lambda} \cdot \mathbf{f}(\mathbf{x}')| \right] \\ &\leq 2\mathbb{E}_n \left[\max_{\mathbf{x}' \in \mathcal{X}} \|\mathbf{f}(\mathbf{x}')\|_1 \right] \\ &\leq 2 \sum_{m=1}^M \mathbb{E}_n \left[\max_{\mathbf{x}' \in \mathcal{X}} |f_m(\mathbf{x}')| \right] < \infty. \end{aligned}$$

The final inequality here follows since each f_m has continuous sample paths and \mathcal{X} is compact. For example, use Theorem 2.9 from (Azaïš & Wschebor, 2009) and note that for any m and any $\mathbf{x} \in \mathcal{X}$, we have $\mathbb{E}_n[\max_{\mathbf{x}' \in \mathcal{X}} |f_m(\mathbf{x}')|] \leq 2\mathbb{E}_n[\max_{\mathbf{x}' \in \mathcal{X}} f_m(\mathbf{x}')] + \mathbb{E}_n|f_m(\mathbf{x})|$.

To show the same for \bar{H}_n , we simply take expectation over $\boldsymbol{\lambda} \sim p(\boldsymbol{\lambda})$. That is,

$$\bar{H}_n = \mathbb{E}_{\boldsymbol{\lambda} \sim p(\boldsymbol{\lambda})}[H_n(\boldsymbol{\lambda})] \leq \sum_{m=1}^M \mathbb{E}_n \left[\sup_{\mathbf{x} \in \mathcal{X}} |f_m(\mathbf{x})| \right] < \infty.$$

□

Remark A.3. Consider the case of random scalarizations. Since \mathbf{x}_{n+1} and m_{n+1} are deterministic after conditioning on \mathcal{F}_n ,³ we can substitute them directly inside the outer expectation in $\alpha_{\text{C-MOKG}}^n(\mathbf{x}_{n+1}, m_{n+1}; \boldsymbol{\lambda}_{n+1}, \mathbf{c})$. Further, for all $\mathbf{x}' \in \mathcal{X}$,

²Note that in (Bect et al., 2019), the character ε is used in place of η

³Formally, we say that \mathbf{x}_{n+1} and m_{n+1} are \mathcal{F}_n -measurable.

$\mu_{n+}^s(\mathbf{x}'; \mathbf{x}_{n+1}, m_{n+1}, \boldsymbol{\lambda}_{n+1}) = \mu_{n+1}^s(\mathbf{x}'; \boldsymbol{\lambda}_{n+1})$ and we have

$$\begin{aligned} \alpha_{\text{C-MOKG}}^n(\mathbf{x}_{n+1}, m_{n+1}; \boldsymbol{\lambda}_{n+1}, \mathbf{c}) &= \frac{1}{c_{m_{n+1}}} \left(\mathbb{E}_n \left[\max_{\mathbf{x}' \in \mathcal{X}} \mu_{n+1}^s(\mathbf{x}'; \boldsymbol{\lambda}_{n+1}) \right] - \max_{\mathbf{x}' \in \mathcal{X}} \mu_n^s(\mathbf{x}'; \boldsymbol{\lambda}_{n+1}) \right) \\ &= \frac{1}{c_{m_{n+1}}} \left(\mathbb{E}_n \left[\max_{\mathbf{x}' \in \mathcal{X}} \mathbb{E}_{n+1} [\boldsymbol{\lambda}_{n+1} \cdot \mathbf{f}(\mathbf{x}')] \right] - \max_{\mathbf{x}' \in \mathcal{X}} \mathbb{E}_n [\boldsymbol{\lambda}_{n+1} \cdot \mathbf{f}(\mathbf{x}')] \right) \\ &= \frac{1}{c_{m_{n+1}}} \left(H_n(\boldsymbol{\lambda}_{n+1}) - \mathbb{E}_n [H_{n+1}(\boldsymbol{\lambda}_{n+1})] \right) \quad \text{a.s.} \end{aligned} \quad (24)$$

We obtain a similar result for the case of average scalarizations, giving

$$\bar{\alpha}_{\text{C-MOKG}}^n(\mathbf{x}_{n+1}, m_{n+1}; \mathbf{c}) = \mathbb{E}_{\boldsymbol{\lambda} \sim p(\boldsymbol{\lambda})} [\alpha_{\text{C-MOKG}}^n(\mathbf{x}_{n+1}, m_{n+1}, \boldsymbol{\lambda}; \mathbf{c})] = \frac{1}{c_{m_{n+1}}} \left(\bar{H}_n - \mathbb{E}_n [\bar{H}_{n+1}] \right) \quad \text{a.s.} \quad (25)$$

We begin with three closely related lemmas.

Lemma A.4 (Restatement of Lemma 3.1 from the main text). *Both forms of the C-MOKG are non-negative. That is, for all $n \in \mathbb{N}_0$, $\mathbf{x} \in \mathcal{X}$, $m \in \{1, \dots, M\}$ and all $\boldsymbol{\lambda} \in \Lambda$,*

$$\alpha_{\text{C-MOKG}}^n(\mathbf{x}, m; \boldsymbol{\lambda}, \mathbf{c}) \geq 0 \quad \text{a.s.} \quad \text{and} \quad \bar{\alpha}_{\text{C-MOKG}}^n(\mathbf{x}, m; \mathbf{c}) \geq 0 \quad \text{a.s.}$$

Proof. We first prove the result for $\alpha_{\text{C-MOKG}}^n(\cdot, \cdot; \boldsymbol{\lambda}, \mathbf{c})$, which takes the scalarization weights $\boldsymbol{\lambda}$ as an argument. Let $n \in \mathbb{N}_0$, $\mathbf{x} \in \mathcal{X}$, $m \in \{1, \dots, M\}$ and let $\boldsymbol{\lambda} \in \Lambda$ be random. Then, for any $\mathbf{x}'' \in \mathcal{X}$,

$$\max_{\mathbf{x}' \in \mathcal{X}} \mu_{n+}^s(\mathbf{x}'; \mathbf{x}, m, \boldsymbol{\lambda}) \geq \mu_{n+}^s(\mathbf{x}''; \mathbf{x}, m, \boldsymbol{\lambda}).$$

Taking expectation conditional on \mathcal{F}_n and $\boldsymbol{\lambda}$ using \mathbb{E}_n gives

$$\mathbb{E}_n \left[\max_{\mathbf{x}' \in \mathcal{X}} \mu_{n+}^s(\mathbf{x}'; \mathbf{x}, m, \boldsymbol{\lambda}) \right] \geq \mathbb{E}_n [\mu_{n+}^s(\mathbf{x}''; \mathbf{x}, m, \boldsymbol{\lambda})] = \mu_n^s(\mathbf{x}''; \boldsymbol{\lambda}).$$

Finally, this holds for all $\mathbf{x}'' \in \mathcal{X}$ so certainly holds for the maximum

$$\begin{aligned} \mathbb{E}_n \left[\max_{\mathbf{x}' \in \mathcal{X}} \mu_{n+}^s(\mathbf{x}'; \mathbf{x}, m, \boldsymbol{\lambda}) \right] &\geq \max_{\mathbf{x}' \in \mathcal{X}} \mu_n^s(\mathbf{x}'; \boldsymbol{\lambda}) \\ \Rightarrow \alpha_{\text{C-MOKG}}^n(\mathbf{x}, m; \boldsymbol{\lambda}, \mathbf{c}) &= \frac{1}{c_m} \left(\mathbb{E}_n \left[\max_{\mathbf{x}' \in \mathcal{X}} \mu_{n+}^s(\mathbf{x}'; \mathbf{x}, m, \boldsymbol{\lambda}) \right] - \max_{\mathbf{x}' \in \mathcal{X}} \mu_n^s(\mathbf{x}'; \boldsymbol{\lambda}) \right) \geq 0 \end{aligned}$$

To show the result for $\bar{\alpha}_{\text{C-MOKG}}$, we simply take expectation to integrate out $\boldsymbol{\lambda}$,

$$\bar{\alpha}_{\text{C-MOKG}}^n(\mathbf{x}, m; \mathbf{c}) = \mathbb{E}_{\boldsymbol{\lambda} \sim p(\boldsymbol{\lambda})} [\alpha_{\text{C-MOKG}}^n(\mathbf{x}, m; \boldsymbol{\lambda}, \mathbf{c})] \geq 0. \quad \square$$

Lemma A.5. *In both cases, the residual uncertainty is at least the C-MOKG scaled by the objective cost. That is, for all $n \in \mathbb{N}_0$, $\mathbf{x} \in \mathcal{X}$, $m \in \{1, \dots, M\}$ and all $\boldsymbol{\lambda} \in \Lambda$,*

$$c_m \alpha_{\text{C-MOKG}}^n(\mathbf{x}, m; \boldsymbol{\lambda}, \mathbf{c}) \leq H_n(\boldsymbol{\lambda}) \quad \text{and} \quad c_m \bar{\alpha}_{\text{C-MOKG}}^n(\mathbf{x}, m; \mathbf{c}) \leq \bar{H}_n.$$

Proof. Let $\boldsymbol{\lambda} \in \Lambda$. By a very similar argument as was used to show that the C-MOKG was non-negative in Lemma A.4,

$$\begin{aligned} \forall \mathbf{x}'' \in \mathcal{X}, \quad & \max_{\mathbf{x}' \in \mathcal{X}} \boldsymbol{\lambda} \cdot \mathbf{f}(\mathbf{x}') \geq \boldsymbol{\lambda} \cdot \mathbf{f}(\mathbf{x}'') \\ \Rightarrow \forall n \in \mathbb{N}_0 \forall \mathbf{x}'' \in \mathcal{X}, \quad & \mathbb{E}_n \left[\max_{\mathbf{x}' \in \mathcal{X}} \boldsymbol{\lambda} \cdot \mathbf{f}(\mathbf{x}') \mid y_m^{\mathbf{x}} \right] \geq \mathbb{E}_n [\boldsymbol{\lambda} \cdot \mathbf{f}(\mathbf{x}'') \mid y_m^{\mathbf{x}}] = \mu_{n+}^s(\mathbf{x}''; \mathbf{x}, m, \boldsymbol{\lambda}) \\ \Rightarrow \quad & \forall n \in \mathbb{N}_0, \quad \mathbb{E}_n \left[\max_{\mathbf{x}' \in \mathcal{X}} \boldsymbol{\lambda} \cdot \mathbf{f}(\mathbf{x}') \mid y_m^{\mathbf{x}} \right] \geq \max_{\mathbf{x}' \in \mathcal{X}} \mu_{n+}^s(\mathbf{x}'; \mathbf{x}, m, \boldsymbol{\lambda}) \\ \Rightarrow \quad & \forall n \in \mathbb{N}_0, \quad \mathbb{E}_n \left[\max_{\mathbf{x}' \in \mathcal{X}} \boldsymbol{\lambda} \cdot \mathbf{f}(\mathbf{x}') \right] \geq \mathbb{E}_n \left[\max_{\mathbf{x}' \in \mathcal{X}} \mu_{n+}^s(\mathbf{x}'; \mathbf{x}, m, \boldsymbol{\lambda}) \right] \\ \Rightarrow \quad & \forall n \in \mathbb{N}_0, \quad H_n(\boldsymbol{\lambda}) \geq c_m \alpha_{\text{C-MOKG}}^n(\mathbf{x}, m; \boldsymbol{\lambda}, \mathbf{c}). \end{aligned}$$

To establish that $\bar{H}_n \geq c_m \bar{\alpha}_{\text{C-MOKG}}^n(\mathbf{x}, m; \mathbf{c})$, we simply take expectation over $\boldsymbol{\lambda} \sim p(\Lambda)$. \square

Lemma A.6. For all $\boldsymbol{\lambda} \in \Lambda$, the sequence $(H_n(\boldsymbol{\lambda}))_{n \in \mathbb{N}_0}$ is a non-negative supermartingale with respect to the filtration $(\mathcal{F}_n)_{n=0}^\infty$. Similarly, $(\bar{H}_n)_{n \in \mathbb{N}_0}$ is a non-negative supermartingale with respect to the same filtration. That is,

$$\begin{aligned} \forall \boldsymbol{\lambda} \in \Lambda \quad \forall n \in \mathbb{N}_0, \quad H_n(\boldsymbol{\lambda}) \geq 0 \text{ a.s.} \quad & \text{and} \quad H_n(\boldsymbol{\lambda}) \geq \mathbb{E}_n[H_{n+1}(\boldsymbol{\lambda})] \text{ a.s.} \\ \forall n \in \mathbb{N}_0, \quad \bar{H}_n \geq 0 \text{ a.s.} \quad & \text{and} \quad \bar{H}_n \geq \mathbb{E}_n[\bar{H}_{n+1}] \text{ a.s.} \end{aligned}$$

Proof. Let $\boldsymbol{\lambda} \in \Lambda$. By Lemmas A.4 and A.5, for all $\boldsymbol{x} \in \mathcal{X}$ and all $m \in \{1, \dots, M\}$,

$$H_n(\boldsymbol{\lambda}) \geq c_m \alpha_{\text{C-MOKG}}^n(\boldsymbol{x}, m; \boldsymbol{\lambda}, \boldsymbol{c}) \geq 0 \quad \text{and} \quad \bar{H}_n \geq c_m \bar{\alpha}_{\text{C-MOKG}}^n(\boldsymbol{x}, m; \boldsymbol{c}) \geq 0$$

almost surely. Further, by a similar argument used to prove Lemmas A.4 and A.5, for all $n \in \mathbb{N}_0$,

$$\begin{aligned} & \forall \boldsymbol{x}'' \in \mathcal{X}, \quad \max_{\boldsymbol{x}'} \mathbb{E}_{n+1}[\boldsymbol{\lambda} \cdot \boldsymbol{f}(\boldsymbol{x}')] \geq \mathbb{E}_{n+1}[\boldsymbol{\lambda} \cdot \boldsymbol{f}(\boldsymbol{x}'')] \\ \Rightarrow & \forall \boldsymbol{x}'' \in \mathcal{X}, \quad \mathbb{E}_n \left[\max_{\boldsymbol{x}' \in \mathcal{X}} \mathbb{E}_{n+1}[\boldsymbol{\lambda} \cdot \boldsymbol{f}(\boldsymbol{x}')] \right] \geq \mathbb{E}_n[\boldsymbol{\lambda} \cdot \boldsymbol{f}(\boldsymbol{x}'')] \\ \Rightarrow & \mathbb{E}_n \left[\max_{\boldsymbol{x}' \in \mathcal{X}} \mathbb{E}_{n+1}[\boldsymbol{\lambda} \cdot \boldsymbol{f}(\boldsymbol{x}')] \right] \geq \max_{\boldsymbol{x}' \in \mathcal{X}} \mathbb{E}_n[\boldsymbol{\lambda} \cdot \boldsymbol{f}(\boldsymbol{x}')] \\ \Rightarrow & \mathbb{E}_n[H_{n+1}(\boldsymbol{\lambda})] \leq H_n(\boldsymbol{\lambda}). \end{aligned}$$

Taking expectation over $\boldsymbol{\lambda} \sim p(\boldsymbol{\lambda})$ gives the result for \bar{H}_n . □

Next, we establish a Lipschitz property of the C-MOKG and residual uncertainty.

Lemma A.7. The C-MOKG and residual uncertainty exhibit the following Lipschitz style properties in $\boldsymbol{\lambda} \in \Lambda$, which hold almost surely. Let $\boldsymbol{\lambda}, \boldsymbol{\lambda}' \in \Lambda$ and $n \in \mathbb{N}_0$. Then

1. for all $\boldsymbol{x} \in \mathcal{X}$ and $m \in \{1, \dots, M\}$,

$$\left| \alpha_{\text{C-MOKG}}^n(\boldsymbol{x}, m; \boldsymbol{\lambda}, \boldsymbol{c}) - \alpha_{\text{C-MOKG}}^n(\boldsymbol{x}, m; \boldsymbol{\lambda}', \boldsymbol{c}) \right| \leq \frac{2}{c_m} \|\boldsymbol{\lambda} - \boldsymbol{\lambda}'\|_2 \mathbb{E}_n \left[\max_{\boldsymbol{x}' \in \mathcal{X}} \|\boldsymbol{f}(\boldsymbol{x}')\|_2 \right];$$

2.

$$|H_n(\boldsymbol{\lambda}) - H_n(\boldsymbol{\lambda}')| \leq 2 \|\boldsymbol{\lambda} - \boldsymbol{\lambda}'\|_2 \mathbb{E}_n \left[\max_{\boldsymbol{x}' \in \mathcal{X}} \|\boldsymbol{f}(\boldsymbol{x}')\|_2 \right].$$

Proof. We will begin with the C-MOKG. Let $\boldsymbol{\lambda}, \boldsymbol{\lambda}' \in \Lambda$. Then for all $\boldsymbol{x}, \boldsymbol{x}' \in \mathcal{X}$, $m \in \{1, \dots, M\}$ and $n \in \mathbb{N}_0$,

$$\begin{aligned} \mu_{n+}^s(\boldsymbol{x}'; \boldsymbol{x}, m, \boldsymbol{\lambda}) - \mu_{n+}^s(\boldsymbol{x}'; \boldsymbol{x}, m, \boldsymbol{\lambda}') &= \mathbb{E}_n [(\boldsymbol{\lambda} - \boldsymbol{\lambda}') \cdot \boldsymbol{f}(\boldsymbol{x}') \mid y_m^{\boldsymbol{x}}] \\ &\leq \mathbb{E}_n \left[\|\boldsymbol{\lambda} - \boldsymbol{\lambda}'\|_2 \|\boldsymbol{f}(\boldsymbol{x}')\|_2 \mid y_m^{\boldsymbol{x}} \right] \\ &\leq \|\boldsymbol{\lambda} - \boldsymbol{\lambda}'\|_2 \mathbb{E}_n \left[\max_{\boldsymbol{x}'' \in \mathcal{X}} \|\boldsymbol{f}(\boldsymbol{x}'')\|_2 \mid y_m^{\boldsymbol{x}} \right] \end{aligned}$$

where the second line follows from the Cauchy-Schwarz inequality. We can do similarly for $\mu_n^s(\boldsymbol{x}'; \boldsymbol{\lambda})$, giving

$$\mu_n^s(\boldsymbol{x}'; \boldsymbol{\lambda}') - \mu_n^s(\boldsymbol{x}'; \boldsymbol{\lambda}) \leq \|\boldsymbol{\lambda} - \boldsymbol{\lambda}'\|_2 \mathbb{E}_n \left[\max_{\boldsymbol{x}'' \in \mathcal{X}} \|\boldsymbol{f}(\boldsymbol{x}'')\|_2 \right].$$

Hence,

$$\begin{aligned}
 c_m \left(\alpha_{\text{C-MOKG}}^n(\mathbf{x}, m; \boldsymbol{\lambda}, \mathbf{c}) - \alpha_{\text{C-MOKG}}^n(\mathbf{x}, m; \boldsymbol{\lambda}', \mathbf{c}) \right) &= \mathbb{E}_n \left[\max_{\mathbf{x}' \in \mathcal{X}} \mu_{n+}^s(\mathbf{x}'; \mathbf{x}, m, \boldsymbol{\lambda}) \right] - \max_{\mathbf{x}' \in \mathcal{X}} \mu_n^s(\mathbf{x}'; \boldsymbol{\lambda}) \\
 &\quad - \mathbb{E}_n \left[\max_{\mathbf{x}' \in \mathcal{X}} \mu_{n+}^s(\mathbf{x}'; \mathbf{x}, m, \boldsymbol{\lambda}') \right] + \max_{\mathbf{x}' \in \mathcal{X}} \mu_n^s(\mathbf{x}'; \boldsymbol{\lambda}') \\
 &\leq \mathbb{E}_n \left[\max_{\mathbf{x}' \in \mathcal{X}} \mu_{n+}^s(\mathbf{x}'; \mathbf{x}, m, \boldsymbol{\lambda}) - \mu_{n+}^s(\mathbf{x}'; \mathbf{x}, m, \boldsymbol{\lambda}') \right] + \max_{\mathbf{x}' \in \mathcal{X}} \left(\mu_n^s(\mathbf{x}'; \boldsymbol{\lambda}') - \mu_n^s(\mathbf{x}'; \boldsymbol{\lambda}) \right) \\
 &\leq \mathbb{E}_n \left[\|\boldsymbol{\lambda} - \boldsymbol{\lambda}'\|_2 \mathbb{E}_n \left[\max_{\mathbf{x}' \in \mathcal{X}} \|\mathbf{f}(\mathbf{x}')\|_2 \mid y_m^{\mathbf{x}} \right] \right] + \|\boldsymbol{\lambda} - \boldsymbol{\lambda}'\|_2 \mathbb{E}_n \left[\max_{\mathbf{x}' \in \mathcal{X}} \|\mathbf{f}(\mathbf{x}')\|_2 \right] \\
 &= 2\|\boldsymbol{\lambda} - \boldsymbol{\lambda}'\|_2 \mathbb{E}_n \left[\max_{\mathbf{x}' \in \mathcal{X}} \|\mathbf{f}(\mathbf{x}')\|_2 \right].
 \end{aligned}$$

Since this holds with $\boldsymbol{\lambda}$ and $\boldsymbol{\lambda}'$ interchanged, we have established the inequality for $\alpha_{\text{C-MOKG}}^n$.

The proof for the residual uncertainty is similar. Again, let $\boldsymbol{\lambda}, \boldsymbol{\lambda}' \in \Lambda$. Then for all $n \in \mathbb{N}_0$,

$$\begin{aligned}
 H_n(\boldsymbol{\lambda}) - H_n(\boldsymbol{\lambda}') &= \mathbb{E}_n \left[\max_{\mathbf{x}' \in \mathcal{X}} \boldsymbol{\lambda} \cdot \mathbf{f}(\mathbf{x}') \right] - \max_{\mathbf{x}' \in \mathcal{X}} \mathbb{E}_n[\boldsymbol{\lambda} \cdot \mathbf{f}(\mathbf{x}')] \\
 &\quad - \mathbb{E}_n \left[\max_{\mathbf{x}' \in \mathcal{X}} \boldsymbol{\lambda}' \cdot \mathbf{f}(\mathbf{x}') \right] + \max_{\mathbf{x}' \in \mathcal{X}} \mathbb{E}_n[\boldsymbol{\lambda}' \cdot \mathbf{f}(\mathbf{x}')] \\
 &\leq \mathbb{E}_n \left[\max_{\mathbf{x}' \in \mathcal{X}} (\boldsymbol{\lambda} - \boldsymbol{\lambda}') \cdot \mathbf{f}(\mathbf{x}') \right] + \max_{\mathbf{x}' \in \mathcal{X}} \mathbb{E}_n [(\boldsymbol{\lambda}' - \boldsymbol{\lambda}) \cdot \mathbf{f}(\mathbf{x}')] \\
 &\leq \mathbb{E}_n \left[\max_{\mathbf{x}' \in \mathcal{X}} \|\boldsymbol{\lambda} - \boldsymbol{\lambda}'\|_2 \|\mathbf{f}(\mathbf{x}')\|_2 \right] + \max_{\mathbf{x}' \in \mathcal{X}} \mathbb{E}_n [\|\boldsymbol{\lambda} - \boldsymbol{\lambda}'\|_2 \|\mathbf{f}(\mathbf{x}')\|_2] \\
 &\leq 2\|\boldsymbol{\lambda} - \boldsymbol{\lambda}'\|_2 \mathbb{E}_n \left[\max_{\mathbf{x}' \in \mathcal{X}} \|\mathbf{f}(\mathbf{x}')\|_2 \right].
 \end{aligned}$$

Again, this holds with $\boldsymbol{\lambda}$ and $\boldsymbol{\lambda}'$ interchanged, so establishing the inequality for H_n . \square

We are now in a position to state and prove the first two main results, which show convergence of $\alpha_{\text{C-MOKG}}^n(\mathbf{x}, m; \boldsymbol{\lambda}, \mathbf{c})$ to zero in a certain sense, both when using random scalarizations and expectation over scalarizations.

Theorem A.8. *Suppose we select samples using C-MOKG with random scalarization weights $\boldsymbol{\lambda}_1, \boldsymbol{\lambda}_2, \dots$ chosen independently according to distribution $p(\boldsymbol{\lambda})$. Then,*

$$\forall \boldsymbol{\lambda} \in \Lambda, \quad \mathbb{P} \left(\liminf_{n \rightarrow \infty} \sup_{\mathbf{x} \in \mathcal{X}, m \in [M]} \alpha_{\text{C-MOKG}}^n(\mathbf{x}, m; \boldsymbol{\lambda}, \mathbf{c}) = 0 \right) = 1.$$

Remark A.9. In fact, it is true that for all $\boldsymbol{\lambda} \in \Lambda$, $\sup_{\mathbf{x} \in \mathcal{X}, m \in [M]} \alpha_{\text{C-MOKG}}^n(\mathbf{x}, m; \boldsymbol{\lambda}, \mathbf{c}) \rightarrow 0$ as $n \rightarrow \infty$ almost surely. However, the proof of this will have to wait until Corollary A.15.

Proof. Let $\boldsymbol{\lambda} \in \Lambda$. The proof in the single objective case found in (Bect et al., 2019) rests on the fact that we use the same acquisition function at each step of the optimization. However, for the multi-objective case with random scalarizations $(\boldsymbol{\lambda}_n)_{n=1}^\infty$, we are effectively changing the acquisition function at each step. The key observation which lets us proceed is that, while we will not use the exact weights $\boldsymbol{\lambda}$ infinitely often, we will use weights which are arbitrarily close, infinitely often, and these will be similar enough. Formally, we observe that there exists a (random) subsequence $(\boldsymbol{\lambda}_{1+n_j})_{j=0}^\infty$ with $\boldsymbol{\lambda}_{1+n_j} \rightarrow \boldsymbol{\lambda}$ as $j \rightarrow \infty$ almost surely. Without loss of generality and for the purpose of slightly easing notation later, we will assume $n_0 = 0$. We will first show that $\sup_{\mathbf{x} \in \mathcal{X}, m \in [M]} \alpha_{\text{C-MOKG}}^{n_j}(\mathbf{x}, m; \boldsymbol{\lambda}_{1+n_j}, \mathbf{c}) \rightarrow 0$ almost surely, then use the convergence of the subsequence to assert the same when we replace $\boldsymbol{\lambda}_{1+n_j}$ with $\boldsymbol{\lambda}$.

Inspired by the notation from Bect et al. (2019), for each $j \in \mathbb{N}_0$ let

$$\begin{aligned}\Delta_{j+1}^{(1)} &= H_{n_j}(\boldsymbol{\lambda}_{1+n_j}) - H_{n_{(j+1)}}(\boldsymbol{\lambda}_{1+n_{(j+1)}}), & \bar{\Delta}_{j+1}^{(1)} &= \mathbb{E}_{n_j}[\Delta_{j+1}^{(1)}], \\ \Delta_{j+1}^{(2)} &= H_{n_{(j+1)}}(\boldsymbol{\lambda}_{1+n_{(j+1)}}) - H_{n_{(j+1)}}(\boldsymbol{\lambda}_{1+n_j}), & \bar{\Delta}_{j+1}^{(2)} &= \mathbb{E}_{n_j}[\Delta_{j+1}^{(2)}].\end{aligned}$$

The first pair here give the difference between successive terms in the sequence $(H_{n_j}(\boldsymbol{\lambda}_{1+n_j}))_{j=0}^\infty$ while the second is a correction to ‘undo’ changing $\boldsymbol{\lambda}_{1+n_j}$. Then, using the results we have derived so far,

$$\begin{aligned}\bar{\Delta}_{j+1}^{(1)} + \bar{\Delta}_{j+1}^{(2)} &= H_{n_j}(\boldsymbol{\lambda}_{1+n_j}) - \mathbb{E}_{n_j}[H_{n_{(j+1)}}(\boldsymbol{\lambda}_{1+n_j})] \\ &\geq H_{n_j}(\boldsymbol{\lambda}_{1+n_j}) - \mathbb{E}_{n_j}[H_{1+n_j}(\boldsymbol{\lambda}_{1+n_j})] && \text{since } H_n(\boldsymbol{\lambda}) \text{ is a supermartingale} \\ &= c_{m_{1+n_j}} \alpha_{\text{C-MOKG}}^{n_j}(\mathbf{x}_{1+n_j}, m_{1+n_j}; \boldsymbol{\lambda}_{1+n_j}, \mathbf{c}) && \text{by Equation (24)} \\ &> c_{m_{1+n_j}} \left(\sup_{\mathbf{x} \in \mathcal{X}, m \in [M]} \alpha_{\text{C-MOKG}}^{n_j}(\mathbf{x}, m; \boldsymbol{\lambda}_{1+n_j}, \mathbf{c}) - \eta_{n_j} \right) && \text{by Equation (22a).}\end{aligned}$$

Therefore, if we can show that almost surely $\bar{\Delta}_j^{(1)} \rightarrow 0$ and $\bar{\Delta}_j^{(2)} \rightarrow 0$ as $j \rightarrow \infty$, then we will have almost surely $\sup_{\mathbf{x} \in \mathcal{X}, m \in [M]} \alpha_{\text{C-MOKG}}^{n_j}(\mathbf{x}, m; \boldsymbol{\lambda}_{1+n_j}, \mathbf{c}) \rightarrow 0$.

For any $j \in \mathbb{N}$ we have $\sum_{i=1}^j \Delta_i^{(1)} = H_0(\boldsymbol{\lambda}_1) - H_{n_j}(\boldsymbol{\lambda}_{1+n_j})$. Therefore, since each $H_{n_j}(\boldsymbol{\lambda}_{1+n_j})$ is almost surely non-negative (Lemma A.6),

$$\forall j \in \mathbb{N}, \quad \mathbb{E} \left[\sum_{i=1}^j \bar{\Delta}_i^{(1)} \right] = \mathbb{E} \left[\sum_{i=1}^j \Delta_i^{(1)} \right] = \mathbb{E}[H_0(\boldsymbol{\lambda}_1) - H_{n_j}(\boldsymbol{\lambda}_{1+n_j})] \leq \mathbb{E}[H_0(\boldsymbol{\lambda}_1)] < \infty.$$

Thus $\bar{\Delta}_j^{(1)} \rightarrow 0$ as $j \rightarrow \infty$ almost surely.

To show that $\Delta_j^{(2)} \rightarrow 0$ almost surely, we will use Lemma A.7. Indeed, this gives that, for all j ,

$$\begin{aligned}|\Delta_{j+1}^{(2)}| &= |H_{n_{(j+1)}}(\boldsymbol{\lambda}_{1+n_{(j+1)}}) - H_{n_{(j+1)}}(\boldsymbol{\lambda}_{1+n_j})| \\ &\leq 2 \|\boldsymbol{\lambda}_{1+n_{(j+1)}} - \boldsymbol{\lambda}_{1+n_j}\|_2 \mathbb{E}_{n_{(j+1)}} \left[\max_{\mathbf{x}' \in \mathcal{X}} \|\mathbf{f}(\mathbf{x}')\|_2 \right].\end{aligned}$$

But $\mathbb{E}_{n_{(j+1)}}[\max_{\mathbf{x}' \in \mathcal{X}} \|\mathbf{f}(\mathbf{x}')\|_2] \rightarrow \mathbb{E}_\infty[\max_{\mathbf{x}' \in \mathcal{X}} \|\mathbf{f}(\mathbf{x}')\|_2]$ as $j \rightarrow \infty$ almost surely, by Lévy’s zero-one law. Also, by construction, $\|\boldsymbol{\lambda}_{1+n_{(j+1)}} - \boldsymbol{\lambda}_{1+n_j}\|_2 \rightarrow 0$ as $j \rightarrow \infty$ almost surely. Therefore, $\Delta_j^{(2)} \rightarrow 0$ almost surely.

Whence,

$$0 \leq \sup_{\mathbf{x} \in \mathcal{X}, m \in [M]} \alpha_{\text{C-MOKG}}^{n_j}(\mathbf{x}, m; \boldsymbol{\lambda}_{1+n_j}, \mathbf{c}) < \frac{1}{c_{m_{1+n_j}}} (\Delta_{j+1}^{(1)} + \Delta_{j+1}^{(2)}) + \eta_{n_j} \rightarrow 0$$

as $j \rightarrow \infty$ almost surely.

To show that we can replace the $\boldsymbol{\lambda}_{1+n_j}$ with their limit $\boldsymbol{\lambda}$, observe that for all $j \geq 0$,

$$\begin{aligned}\sup_{\mathbf{x} \in \mathcal{X}, m \in [M]} \alpha_{\text{C-MOKG}}^{n_j}(\mathbf{x}, m; \boldsymbol{\lambda}, \mathbf{c}) &\leq \sup_{\mathbf{x} \in \mathcal{X}, m \in [M]} \alpha_{\text{C-MOKG}}^{n_j}(\mathbf{x}, m; \boldsymbol{\lambda}_{1+n_j}, \mathbf{c}) \\ &\quad + \sup_{\mathbf{x} \in \mathcal{X}, m \in [M]} \left(\alpha_{\text{C-MOKG}}^{n_j}(\mathbf{x}, m; \boldsymbol{\lambda}, \mathbf{c}) - \alpha_{\text{C-MOKG}}^{n_j}(\mathbf{x}, m; \boldsymbol{\lambda}_{1+n_j}, \mathbf{c}) \right) \\ &\leq \underbrace{\sup_{\mathbf{x} \in \mathcal{X}, m \in [M]} \alpha_{\text{C-MOKG}}^{n_j}(\mathbf{x}, m; \boldsymbol{\lambda}_{1+n_j}, \mathbf{c})}_{\rightarrow 0} \\ &\quad + 2 \underbrace{\|\boldsymbol{\lambda} - \boldsymbol{\lambda}_{1+n_j}\|_2}_{\rightarrow 0} \underbrace{\mathbb{E}_{n_j} \left[\max_{\mathbf{x}' \in \mathcal{X}} \|\mathbf{f}(\mathbf{x}')\|_2 \right]}_{\rightarrow \mathbb{E}_\infty[\max_{\mathbf{x}' \in \mathcal{X}} \|\mathbf{f}(\mathbf{x}')\|_2] < \infty} \\ &\rightarrow 0 \quad \text{as } j \rightarrow \infty.\end{aligned}$$

On the penultimate line, we have used that $\max_{\mathbf{x}' \in \mathcal{X}} \|\mathbf{f}(\mathbf{x}')\|_2$ is L^1 -integrable and thus by Lévy's zero-one law the conditional expectations, $\mathbb{E}_{n_j}[\max_{\mathbf{x}' \in \mathcal{X}} \|\mathbf{f}(\mathbf{x}')\|_2]$, converge almost surely to $\mathbb{E}_\infty[\max_{\mathbf{x}' \in \mathcal{X}} \|\mathbf{f}(\mathbf{x}')\|_2] < \infty$.

Therefore, the whole upper bound converges to zero and we conclude that

$$\sup_{\mathbf{x} \in \mathcal{X}, m \in [M]} \alpha_{\text{C-MOKG}}^{n_j}(\mathbf{x}, m; \boldsymbol{\lambda}, \mathbf{c}) \rightarrow 0 \quad \text{as } j \rightarrow \infty \quad \text{a.s.}$$

Hence, $\liminf_{n \rightarrow \infty} \sup_{\mathbf{x} \in \mathcal{X}, m \in [M]} \alpha_{\text{C-MOKG}}^n(\mathbf{x}, m; \boldsymbol{\lambda}, \mathbf{c}) = 0$ almost surely, completing the proof. \square

We also make a similar statement for expectation over scalarization, except for this one we can already replace the limit inferior with a true limit.

Theorem A.10. *Suppose we select samples using C-MOKG with expectation over scalarizations. Then, for all preference vectors $\boldsymbol{\lambda} \in \Lambda$, $\alpha_{\text{C-MOKG}}^n(\mathbf{x}, m; \boldsymbol{\lambda}, \mathbf{c}) \rightarrow 0$ as $n \rightarrow \infty$ uniformly in $\mathbf{x} \in \mathcal{X}$ and $m \in \{1, \dots, M\}$, almost surely. That is,*

$$\forall \boldsymbol{\lambda} \in \Lambda, \quad \mathbb{P} \left(\sup_{\mathbf{x} \in \mathcal{X}, m \in [M]} \alpha_{\text{C-MOKG}}^n(\mathbf{x}, m; \boldsymbol{\lambda}, \mathbf{c}) \rightarrow 0 \quad \text{as } n \rightarrow \infty \right) = 1.$$

Proof. The proof in the case of expectation over scalarizations is simpler than that of Theorem A.8 since we have used the same acquisition function at each step of the optimization.

We will first prove that $\bar{\alpha}_{\text{C-MOKG}}^n(\mathbf{x}, m; \mathbf{c}) \rightarrow 0$ uniformly in $\mathbf{x} \in \mathcal{X}$ and $m \in \{1, 2, \dots, M\}$, almost surely. For each $n \in \mathbb{N}_0$, let us redefine $\Delta_{n+1} = \bar{H}_n - \bar{H}_{n+1}$ and $\bar{\Delta}_{n+1} = \mathbb{E}_n[\Delta_{n+1}]$. As remarked earlier in Equation (25), $\bar{\alpha}_{\text{C-MOKG}}^n(\mathbf{x}_{n+1}, m_{n+1}; \mathbf{c}) = \frac{1}{c_{m_{n+1}}} (\bar{H}_n - \mathbb{E}_n[\bar{H}_{n+1}])$. Therefore, using that \mathbf{x}_{n+1} and m_{n+1} were chosen to maximize $\bar{\alpha}_{\text{C-MOKG}}^n$ according to Equation (22b),

$$\frac{1}{c_{m_{n+1}}} \bar{\Delta}_{n+1} = \frac{1}{c_{m_{n+1}}} (\bar{H}_n - \mathbb{E}_n[\bar{H}_{n+1}]) = \bar{\alpha}_{\text{C-MOKG}}^n(\mathbf{x}_{n+1}, m_{n+1}; \mathbf{c}) > \sup_{\mathbf{x} \in \mathcal{X}, m \in [M]} \bar{\alpha}_{\text{C-MOKG}}^n(\mathbf{x}, m; \mathbf{c}) - \eta_n. \quad (26)$$

Our problem is now reduced to showing that $\bar{\Delta}_n \rightarrow 0$ as $n \rightarrow \infty$. For any $n \in \mathbb{N}_0$ we have $\sum_{j=1}^n \Delta_j = \bar{H}_0 - \bar{H}_n$. Therefore,

$$\forall n \in \mathbb{N}_0, \quad \mathbb{E} \left[\sum_{j=1}^n \bar{\Delta}_j \right] = \mathbb{E} \left[\sum_{j=1}^n \Delta_j \right] = \mathbb{E}[\bar{H}_0 - \bar{H}_n] \leq \mathbb{E}[\bar{H}_0] < \infty$$

where we used Lemma A.6 for the penultimate inequality. Also observe that combining Equation (26) with Lemma A.4 implies $\bar{\Delta}_{n+1} = c_{m_{n+1}} \bar{\alpha}_{\text{C-MOKG}}^n(\mathbf{x}_{n+1}, m_{n+1}; \mathbf{c}) \geq 0$ is almost surely non-negative, so $\bar{\Delta}_{n+1} \rightarrow 0$ as $n \rightarrow \infty$. Hence,

$$0 \leq \sup_{\mathbf{x} \in \mathcal{X}, m \in [M]} \bar{\alpha}_{\text{C-MOKG}}^n(\mathbf{x}, m; \mathbf{c}) < \frac{1}{c_{m_{n+1}}} \bar{\Delta}_{n+1} + \eta_n \rightarrow 0$$

as $n \rightarrow \infty$ almost surely.

We will now use this to show that for all $\boldsymbol{\lambda} \in \Lambda$, $\alpha_{\text{C-MOKG}}^n(\mathbf{x}, m; \boldsymbol{\lambda}, \mathbf{c}) \rightarrow 0$ uniformly in $\mathbf{x} \in \mathcal{X}$ and $m \in \{1, \dots, M\}$, almost surely. Suppose for contradiction that this does not hold. Then there exists $\boldsymbol{\lambda} \in \Lambda$ such that with non-zero probability

$$\limsup_{n \rightarrow \infty} \sup_{\mathbf{x} \in \mathcal{X}, m \in [M]} \alpha_{\text{C-MOKG}}^n(\mathbf{x}, m; \boldsymbol{\lambda}, \mathbf{c}) > 0.$$

By Lemma A.7, for all $\boldsymbol{\lambda}' \in \Lambda$, and all $\mathbf{x} \in \mathcal{X}$, $m \in \{1, \dots, M\}$ and $n \in \mathbb{N}_0$,

$$\alpha_{\text{C-MOKG}}^n(\mathbf{x}, m; \boldsymbol{\lambda}', \mathbf{c}) \geq \alpha_{\text{C-MOKG}}^n(\mathbf{x}, m; \boldsymbol{\lambda}, \mathbf{c}) - \frac{2}{c_m} \|\boldsymbol{\lambda} - \boldsymbol{\lambda}'\|_2 \mathbb{E}_n \left[\max_{\mathbf{x}' \in \mathcal{X}} \|\mathbf{f}(\mathbf{x}')\|_2 \right].$$

Now, $\max_{\mathbf{x}' \in \mathcal{X}} \|\mathbf{f}(\mathbf{x}')\|_2$ is L^1 -integrable and so $\mathbb{E}_n[\max_{\mathbf{x}' \in \mathcal{X}} \|\mathbf{f}(\mathbf{x}')\|_2] \rightarrow \mathbb{E}_\infty[\max_{\mathbf{x}' \in \mathcal{X}} \|\mathbf{f}(\mathbf{x}')\|_2]$ as $n \rightarrow \infty$ almost surely, by Lévy's zero-one law. Therefore, there exists a random $N \in \mathbb{N}_0$ such that, almost surely, for all $n \geq N$, $\mathbb{E}_n[\max_{\mathbf{x}' \in \mathcal{X}} \|\mathbf{f}(\mathbf{x}')\|_2] \leq \frac{3}{2} \mathbb{E}_\infty[\max_{\mathbf{x}' \in \mathcal{X}} \|\mathbf{f}(\mathbf{x}')\|_2]$. That is, we have an upper bound on $\mathbb{E}_n[\max_{\mathbf{x}' \in \mathcal{X}} \|\mathbf{f}(\mathbf{x}')\|_2]$

which is independent of n . Thus there exists a small L^2 -ball $B_\lambda \subset \Lambda$ centered on λ with a strictly positive, random radius such that for all $\lambda' \in B_\lambda$ and $n \geq N$ we have

$$\frac{2}{c_m} \|\lambda - \lambda'\|_2 \mathbb{E}_n \left[\max_{\mathbf{x}' \in \mathcal{X}} \|\mathbf{f}(\mathbf{x}')\|_2 \right] < \min(A_\lambda, 1)$$

where $A_\lambda = \frac{1}{2} \limsup_{n \rightarrow \infty} \sup_{\mathbf{x} \in \mathcal{X}, m \in [M]} \alpha_{\text{C-MOKG}}^n(\mathbf{x}, m; \lambda, \mathbf{c}) > 0$. We have taken the minimum with 1 here to cover the case where $A_\lambda = +\infty$. Thus, for all $n \geq N$ and $\lambda' \in B_\lambda$, and all $\mathbf{x} \in \mathcal{X}$ and $m \in \{1, \dots, M\}$,

$$\alpha_{\text{C-MOKG}}^n(\mathbf{x}, m; \lambda', \mathbf{c}) \geq \alpha_{\text{C-MOKG}}^n(\mathbf{x}, m; \lambda, \mathbf{c}) - \min(A_\lambda, 1).$$

Since C-MOKG is non-negative (Lemma A.4), restricting to B_λ and integrating gives a lower bound on the expectation for all $\mathbf{x} \in \mathcal{X}$, $m \in \{1, \dots, M\}$ and all $n \geq N$,

$$\bar{\alpha}_{\text{C-MOKG}}^n(\mathbf{x}, m; \mathbf{c}) \geq \mathbb{P}(B_\lambda) (\alpha_{\text{C-MOKG}}^n(\mathbf{x}, m; \lambda, \mathbf{c}) - \min(A_\lambda, 1)).$$

Then, taking the supremum and limit gives

$$\begin{aligned} \limsup_{n \rightarrow \infty} \sup_{\mathbf{x} \in \mathcal{X}, m \in [M]} \bar{\alpha}_{\text{C-MOKG}}^n(\mathbf{x}, m; \mathbf{c}) &\geq \mathbb{P}(B_\lambda) \left(\limsup_{n \rightarrow \infty} \sup_{\mathbf{x} \in \mathcal{X}, m \in [M]} \alpha_{\text{C-MOKG}}^n(\mathbf{x}, m; \lambda, \mathbf{c}) - \min(A_\lambda, 1) \right) \\ &\geq \frac{1}{2} \mathbb{P}(B_\lambda) \limsup_{n \rightarrow \infty} \sup_{\mathbf{x} \in \mathcal{X}, m \in [M]} \alpha_{\text{C-MOKG}}^n(\mathbf{x}, m; \lambda, \mathbf{c}) \\ &> 0. \end{aligned}$$

By choice of λ , and because the distribution over Λ is strictly positive, the final strict inequality holds with non-zero probability. Hence we have a contradiction and so we conclude that for all $\lambda \in \Lambda$, $\sup_{\mathbf{x} \in \mathcal{X}, m \in [M]} \alpha_{\text{C-MOKG}}^n(\mathbf{x}, m; \lambda, \mathbf{c}) \rightarrow 0$ as $n \rightarrow \infty$ almost surely. \square

A.3. Convergence to Optimal Recommendations

We have shown that, for each of the two acquisition functions, the limit inferior of $\alpha_{\text{C-MOKG}}^n(\cdot, \cdot; \lambda, \mathbf{c})$, is zero almost surely for each $\lambda \in \Lambda$. In fact, for $\bar{\alpha}_{\text{C-MOKG}}^n$ we have shown almost sure, uniform convergence to 0. However, our aim is a much stronger result.

Recall Equation (15) from the main text, which we restate here as Equation (27). For each $n \in \mathbb{N}_0$ and each preference vector $\lambda \in \Lambda$, let

$$\mathbf{x}_{n,\lambda}^* \in \arg \max_{\mathbf{x} \in \mathcal{X}} \mathbb{E}_n[\lambda \cdot \mathbf{f}(\mathbf{x})] \quad (27)$$

be a random variable which maximizes the posterior mean of the scalarized objective at stage n . Thus, assuming no model mismatch, $\lambda \cdot \mathbf{f}(\mathbf{x}_{1,\lambda}^*), \lambda \cdot \mathbf{f}(\mathbf{x}_{2,\lambda}^*), \dots$ is the sequence of (noiseless) scalarized objective values we would obtain if we were to use the recommended point at each stage of the optimization. Presented for the single-objective case as Proposition 4.9 in (Bect et al., 2019), the next theorem tells us that, this sequence converges to the true maximum of the scalarized, hidden objective function, $\lambda \cdot \mathbf{f}$.

Theorem A.11 (Restatement of Theorem 3.2 from the main text). *Define the $\mathbf{x}_{n,\lambda}^*$ as in Equation (27). When using C-MOKG with either random scalarizations, or expectation over scalarizations, we have*

$$\forall \lambda \in \Lambda, \quad \lambda \cdot \mathbf{f}(\mathbf{x}_{n,\lambda}^*) \rightarrow \max_{\mathbf{x} \in \mathcal{X}} \lambda \cdot \mathbf{f}(\mathbf{x}) \quad \text{as } n \rightarrow \infty$$

almost surely and in mean.

Before showing this, we will first prove an important result establishing almost sure, uniform convergence of the posterior mean and covariance functions of the GP surrogate model, regardless of the acquisition function used. This will be invaluable in proving Theorem A.11.

Let $\mathcal{F}_\infty = \sigma(\cup_{n=0}^\infty \mathcal{F}_n)$ be the smallest σ -algebra containing all the \mathcal{F}_n and let $\mathbb{E}_\infty[\cdot] = \mathbb{E}[\cdot | \mathcal{F}_\infty]$ denote expectation conditional on all observations and choices. Also define conditional mean and covariance functions of \mathbf{f} at each stage,

$$\begin{aligned} \boldsymbol{\mu}_n : \mathcal{X} &\rightarrow \mathbb{R}^M & \mathbf{K}_n : \mathcal{X} \times \mathcal{X} &\rightarrow \mathbb{R}^{M \times M} \\ \mathbf{x} &\mapsto \mathbb{E}_n[\mathbf{f}(\mathbf{x})] & (\mathbf{x}, \mathbf{x}') &\mapsto \mathbb{E}_n[\mathbf{f}(\mathbf{x})\mathbf{f}(\mathbf{x}')^T] - \mathbb{E}_n[\mathbf{f}(\mathbf{x})]\mathbb{E}_n[\mathbf{f}(\mathbf{x}')^T] \\ \boldsymbol{\mu}_\infty : \mathcal{X} &\rightarrow \mathbb{R}^M & \mathbf{K}_\infty : \mathcal{X} \times \mathcal{X} &\rightarrow \mathbb{R}^{M \times M} \\ \mathbf{x} &\mapsto \mathbb{E}_\infty[\mathbf{f}(\mathbf{x})] & (\mathbf{x}, \mathbf{x}') &\mapsto \mathbb{E}_\infty[\mathbf{f}(\mathbf{x})\mathbf{f}(\mathbf{x}')^T] - \mathbb{E}_\infty[\mathbf{f}(\mathbf{x})]\mathbb{E}_\infty[\mathbf{f}(\mathbf{x}')^T] \end{aligned}$$

Note that these are vector- and matrix-valued stochastic processes.

Proposition A.12. *For any choice of query locations $(\mathbf{x}_n, m_n)_{n=1}^\infty$, the sequences of stochastic processes $\boldsymbol{\mu}_n \rightarrow \boldsymbol{\mu}_\infty$ and $\mathbf{K}_n \rightarrow \mathbf{K}_\infty$ converge uniformly as $n \rightarrow \infty$, both almost surely and in L^p for all $1 \leq p < \infty$. Furthermore, the limits $\boldsymbol{\mu}_\infty$ and \mathbf{K}_∞ are continuous.*

Proof. Since \mathcal{X} is compact, the space $\mathcal{C}(\mathcal{X}, \mathbb{R}^M)$ of continuous functions $\mathcal{X} \rightarrow \mathbb{R}^M$ forms a Banach space when equipped with the supremum norm $\|\cdot\|_\infty$. The multi-output Gaussian process \mathbf{f} has continuous sample paths and so can be viewed as a random element of this space. It is also L^p -integrable for any $1 \leq p < \infty$. Indeed, all moments of $\sup_{\mathbf{x} \in \mathcal{X}, m \in [M]} |f_m(\mathbf{x})|$ are finite⁴ and so

$$\|\mathbf{f}\|_{L^p(\mathcal{C}(\mathcal{X}, \mathbb{R}^M))} = \mathbb{E}[\|\mathbf{f}\|_\infty^p]^{1/p} = \mathbb{E}\left[\left(\sup_{\mathbf{x} \in \mathcal{X}, m \in [M]} |f_m(\mathbf{x})|\right)^p\right]^{1/p} < \infty.$$

Observe that the conditional means $\boldsymbol{\mu}_n = \mathbb{E}_n[\mathbf{f}]$ and $\boldsymbol{\mu}_\infty = \mathbb{E}_\infty[\mathbf{f}]$ are continuous since Banach spaces are closed under taking conditional expectation (see e.g. Proposition 1.10 from (Pisier, 2016)). In fact, we have shown that they are a martingale of the form in Theorems 1.14 and 1.30 in (Pisier, 2016), and so $\boldsymbol{\mu}_n \rightarrow \boldsymbol{\mu}_\infty$ almost surely and in L^p . This is a convergence in the function space $\mathcal{C}(\mathcal{X}, \mathbb{R}^M)$ using the supremum norm, which is equivalent to saying that the convergence of the processes is uniform. That is, $\boldsymbol{\mu}_n \rightarrow \boldsymbol{\mu}_\infty$ uniformly, both almost surely and in L^p for any $1 \leq p < \infty$.

We may use the same argument on the sequence of second moments, $\mathbf{M}_n^{(2)}(\mathbf{x}, \mathbf{x}') = \mathbb{E}_n[\mathbf{f}(\mathbf{x})\mathbf{f}(\mathbf{x}')^T]$, in the Banach space $\mathcal{C}(\mathcal{X} \times \mathcal{X}, \mathbb{R}^{M \times M})$. The process $\mathbf{F}^{(2)} \in \mathcal{C}(\mathcal{X} \times \mathcal{X}, \mathbb{R}^{M \times M})$ defined by $\mathbf{F}^{(2)}(\mathbf{x}, \mathbf{x}') = \mathbf{f}(\mathbf{x})\mathbf{f}(\mathbf{x}')^T$ is L^p -integrable for all $1 \leq p < \infty$ since

$$\begin{aligned} \|\mathbf{F}^{(2)}\|_{L^p(\mathcal{C}(\mathcal{X} \times \mathcal{X}, \mathbb{R}^{M \times M}))} &= \mathbb{E}\left[\left(\sup_{\substack{\mathbf{x}, \mathbf{x}' \in \mathcal{X} \\ m, m' \in [M]}} |f_m(\mathbf{x})f_{m'}(\mathbf{x}')|\right)^p\right]^{1/p} \\ &= \mathbb{E}\left[\left(\sup_{\mathbf{x} \in \mathcal{X}, m \in [M]} |f_m(\mathbf{x})|\right)^{2p}\right]^{1/p} = \|\mathbf{f}\|_{L^{2p}(\mathcal{C}(\mathcal{X}, \mathbb{R}^M))}^2 < \infty. \end{aligned}$$

Therefore, we may again apply martingale convergence Theorems 1.14 and 1.30 from (Pisier, 2016) to conclude that $\mathbf{M}_n^{(2)} \rightarrow \mathbf{M}_\infty^{(2)}$ almost surely and in L^p , where $\mathbf{M}_\infty^{(2)}(\mathbf{x}, \mathbf{x}') = \mathbb{E}_\infty[\mathbf{f}(\mathbf{x})\mathbf{f}(\mathbf{x}')^T]$. Since

$$\forall n \in \mathbb{N} \cup \{\infty\} \forall \mathbf{x}, \mathbf{x}' \in \mathcal{X}, \quad \mathbf{K}_n(\mathbf{x}, \mathbf{x}') = \mathbf{M}_n^{(2)}(\mathbf{x}, \mathbf{x}') - \boldsymbol{\mu}_n(\mathbf{x})\boldsymbol{\mu}_n(\mathbf{x}')^T,$$

we conclude that $\mathbf{K}_n \rightarrow \mathbf{K}_\infty$ uniformly, both almost surely and in L^p for all $1 \leq p < \infty$. By the same argument as before, the $\mathbf{M}_n^{(2)}$ and $\mathbf{M}_\infty^{(2)}$ are continuous as conditional expectations of random elements in the Banach space of continuous functions. So the \mathbf{K}_n and \mathbf{K}_∞ are also continuous. \square

Our strategy to prove Theorem A.11 will be to first show that the limiting estimate, $\boldsymbol{\mu}_\infty$, approximates the objective \mathbf{f} up to a constant almost surely. That is, we will show that $\mathbf{f} - \boldsymbol{\mu}_\infty$ has almost surely constant sample paths. The intuition then is that knowledge of $\boldsymbol{\mu}_\infty$ is sufficient to determine the location of the maximum of \mathbf{f} . To show that $\mathbf{f} - \boldsymbol{\mu}_\infty$ has almost surely constant sample paths, we will first show that the limiting covariance function, \mathbf{K}_∞ , has almost surely constant sample paths.

⁴see for example Equation 2.34 in (Azaïs & Wschebor, 2009) and view \mathbf{f} as an \mathbb{R} -valued GP on input space $\mathcal{X} \times [M]$

Lemma A.13. *The limiting covariance function $\mathbf{K}_\infty : \mathcal{X} \times \mathcal{X} \rightarrow \mathbb{R}^{M \times M}$ has almost surely constant sample paths. That is,*

$$\mathbb{P}(\forall \mathbf{x}, \mathbf{u}, \mathbf{x}', \mathbf{u}' \in \mathcal{X}, \quad \mathbf{K}_\infty(\mathbf{u}, \mathbf{x}) = \mathbf{K}_\infty(\mathbf{u}', \mathbf{x}')) = 1.$$

Proof. This proof makes use of the fact that the scalarizations are linear and thus commute with the expectation operator.

Let $\mathbf{x} \in \mathcal{X}$, $m \in \{1, \dots, M\}$ and $\boldsymbol{\lambda} \in \Lambda$. For each $n \in \mathbb{N}_0$ and $\mathbf{u} \in \mathcal{X}$ let

$$\begin{aligned} W_{n,\mathbf{u}} &= \mathbb{E}_n[\boldsymbol{\lambda} \cdot \mathbf{f}(\mathbf{u}) | y_m^{\mathbf{x}}] - \mathbb{E}_n[\boldsymbol{\lambda} \cdot \mathbf{f}(\mathbf{x}_{n,\boldsymbol{\lambda}}^*) | y_m^{\mathbf{x}}] \\ &= \boldsymbol{\lambda} \cdot \mathbb{E}_n[\mathbf{f}(\mathbf{u}) | y_m^{\mathbf{x}}] - \boldsymbol{\lambda} \cdot \mathbb{E}_n[\mathbf{f}(\mathbf{x}_{n,\boldsymbol{\lambda}}^*) | y_m^{\mathbf{x}}]. \end{aligned}$$

Observe that $\alpha_{\mathcal{C}\text{-MOKG}}^n(\mathbf{x}, m; \boldsymbol{\lambda}, \mathbf{c}) = \frac{1}{c_m} \mathbb{E}_n[\sup_{\mathbf{x}' \in \mathcal{X}} W_{n,\mathbf{x}'}]$.

Let $n \in \mathbb{N}_0$ and $\mathbf{u} \in \mathcal{X}$. Since $\sup_{\mathbf{x}' \in \mathcal{X}} W_{n,\mathbf{x}'} \geq 0$, we have

$$\begin{aligned} \sup_{\mathbf{x}' \in \mathcal{X}} W_{n,\mathbf{x}'} &= \sup_{\mathbf{x}' \in \mathcal{X}} \max(W_{n,\mathbf{x}'}, 0) \\ \Rightarrow \quad 0 &\leq \mathbb{E}_n[\max(W_{n,\mathbf{u}}, 0)] \leq \mathbb{E}_n \left[\sup_{\mathbf{x}' \in \mathcal{X}} \max(W_{n,\mathbf{x}'}, 0) \right] = c_m \alpha_{\mathcal{C}\text{-MOKG}}^n(\mathbf{x}, m; \boldsymbol{\lambda}, \mathbf{c}). \end{aligned}$$

Applying Theorem A.8 or Theorem A.10 depending on the acquisition strategy, we have almost surely $\liminf_{n \rightarrow \infty} \sup_{\mathbf{x} \in \mathcal{X}, m \in [M]} \alpha_{\mathcal{C}\text{-MOKG}}^n(\mathbf{x}, m; \boldsymbol{\lambda}, \mathbf{c}) = 0$. Therefore, $\liminf_{n \rightarrow \infty} \mathbb{E}_n[\max(W_{n,\mathbf{u}}, 0)] = 0$ almost surely. This implies that, almost surely,

$$\forall \delta > 0, \quad \liminf_{n \rightarrow \infty} \mathbb{P}_n(W_{n,\mathbf{u}} > \delta) = 0, \quad (28)$$

a statement closely resembling the definition of convergence in probability. Here, the (random) distribution \mathbb{P}_n is defined as the conditional expectation of the indicator variables. That is, for every event $A \in \mathcal{F}$, $\mathbb{P}_n(A) = \mathbb{E}_n[\mathbb{I}_A]$. Writing $\mathbf{k}_{\infty, :, m}$ for the m^{th} column of \mathbf{K}_∞ , we will use Equation (28) to show that

$$\boldsymbol{\lambda} \cdot \mathbf{k}_{\infty, :, m}(\mathbf{u}, \mathbf{x}) = \boldsymbol{\lambda} \cdot \mathbf{k}_{\infty, :, m}(\mathbf{x}, \mathbf{x}) \quad (29)$$

almost surely – something made significantly easier by noting that $W_{n,\mathbf{u}}$ is a Gaussian variable.

Write $k_{n,m,m}$ for the $(m, m)^{\text{th}}$ element of \mathbf{K}_n . If $k_{n,m,m}(\mathbf{x}, \mathbf{x}) = 0$ then $k_{n',m,m}(\mathbf{x}, \mathbf{x}) = 0$ for all $n' \geq n$ and, by Cauchy-Schwarz, $k_{n',m',m}(\mathbf{u}, \mathbf{x}) = 0$ for all $m' \in \{1, \dots, M\}$ and all $n' \geq n$ as well. Hence, $\mathbf{k}_{n, :, m}(\mathbf{u}, \mathbf{x}) - \mathbf{k}_{n, :, m}(\mathbf{x}, \mathbf{x}) = 0$ for all sufficiently large n and so applying Proposition A.12 we have established Equation (29).

So we focus on the event where $k_{n,m,m}(\mathbf{x}, \mathbf{x}) > 0$ for all n . Using the formula for the conditional mean of a Gaussian process in Equation (4), we can express $W_{n,\mathbf{u}}$ as

$$W_{n,\mathbf{u}} = \boldsymbol{\lambda} \cdot \left(\boldsymbol{\mu}_n(\mathbf{u}) - \boldsymbol{\mu}_n(\mathbf{x}_{n,\boldsymbol{\lambda}}^*) + \frac{\mathbf{k}_{n, :, m}(\mathbf{u}, \mathbf{x}) - \mathbf{k}_{n, :, m}(\mathbf{x}_{n,\boldsymbol{\lambda}}^*, \mathbf{x})}{k_{n,m,m}(\mathbf{x}, \mathbf{x}) + \sigma_m^2} (y_m^{\mathbf{x}} - \boldsymbol{\mu}_n(\mathbf{x})) \right)$$

where $y_m^{\mathbf{x}} \sim \mathcal{N}(\boldsymbol{\mu}_n(\mathbf{x}), k_{n,m,m}(\mathbf{x}, \mathbf{x}) + \sigma_m^2)$ is the (random) value observed when we sample the m^{th} objective at \mathbf{x} . Hence, conditional on \mathcal{F}_n , the variable $W_{n,\mathbf{u}}$ itself follows a normal distribution with mean and covariance given by

$$\mathbb{E}_n[W_{n,\mathbf{u}}] = \boldsymbol{\lambda} \cdot (\boldsymbol{\mu}_n(\mathbf{u}) - \boldsymbol{\mu}_n(\mathbf{x}_{n,\boldsymbol{\lambda}}^*)), \quad \text{Var}_n[W_{n,\mathbf{u}}] = \frac{(\boldsymbol{\lambda} \cdot [\mathbf{k}_{n, :, m}(\mathbf{u}, \mathbf{x}) - \mathbf{k}_{n, :, m}(\mathbf{x}_{n,\boldsymbol{\lambda}}^*, \mathbf{x})])^2}{k_{n,m,m}(\mathbf{x}, \mathbf{x}) + \sigma_m^2}.$$

Whence, for any $\delta > 0$,

$$\mathbb{P}_n(W_{n,\mathbf{u}} > \delta) = 1 - \Phi \left(\frac{\sqrt{k_{n,m,m}(\mathbf{x}, \mathbf{x}) + \sigma_m^2}}{|\boldsymbol{\lambda} \cdot (\mathbf{k}_{n, :, m}(\mathbf{u}, \mathbf{x}) - \mathbf{k}_{n, :, m}(\mathbf{x}_{n,\boldsymbol{\lambda}}^*, \mathbf{x}))|} [\delta - \boldsymbol{\lambda} \cdot (\boldsymbol{\mu}_n(\mathbf{u}) - \boldsymbol{\mu}_n(\mathbf{x}_{n,\boldsymbol{\lambda}}^*))] \right)$$

where Φ is the cumulative density function of a standard normal variable.

We have from Proposition A.12 that $\boldsymbol{\mu}_n \rightarrow \boldsymbol{\mu}_\infty$ uniformly as $n \rightarrow \infty$, almost surely. Further, $\boldsymbol{\mu}_\infty$ is continuous and \mathcal{X} is compact. Therefore, there exists a negative, random variable a (not depending on n) such that, for sufficiently large n , $\mathbb{E}_n[W_{n,\mathbf{u}}] = \boldsymbol{\lambda} \cdot (\boldsymbol{\mu}_n(\mathbf{u}) - \boldsymbol{\mu}_n(\mathbf{x}_{n,\boldsymbol{\lambda}}^*)) > a$ almost surely. For example, take any $a < \min \boldsymbol{\lambda} \cdot \boldsymbol{\mu}_\infty - \max \boldsymbol{\lambda} \cdot \boldsymbol{\mu}_\infty$. Thus,

$$\mathbb{P}_n(W_{n,\mathbf{u}} > \delta) \geq 1 - \Phi \left(\frac{\sqrt{k_{n,m,m}(\mathbf{x}, \mathbf{x}) + \sigma_m^2}}{|\boldsymbol{\lambda} \cdot (\mathbf{k}_{n, :, m}(\mathbf{u}, \mathbf{x}) - \mathbf{k}_{n, :, m}(\mathbf{x}_{n,\boldsymbol{\lambda}}^*, \mathbf{x}))|} (\delta - a) \right).$$

By Equation (28), there exists a (random) subsequence $(n_j)_{j=0}^\infty$ such that $\mathbb{P}_{n_j}(W_{n_j, \mathbf{u}} > \delta) \rightarrow 0$ as $j \rightarrow \infty$ and so $\frac{\sqrt{k_{n_j, :, m}(\mathbf{x}, \mathbf{x}) + \sigma_m^2}}{|\lambda \cdot (\mathbf{k}_{n_j, :, m}(\mathbf{u}, \mathbf{x}) - \mathbf{k}_{n_j, :, m}(\mathbf{x}_{n_j, \lambda}^*, \mathbf{x}))|} \rightarrow \infty$ as $j \rightarrow \infty$. Since $(k_{n, m, m}(\mathbf{x}, \mathbf{x}))_{n=1}^\infty$ is a decreasing sequence, we must therefore have $\lambda \cdot (\mathbf{k}_{n_j, :, m}(\mathbf{u}, \mathbf{x}) - \mathbf{k}_{n_j, :, m}(\mathbf{x}_{n_j, \lambda}^*, \mathbf{x})) \rightarrow 0$ almost surely. This holds for all \mathbf{u} , including the case $\mathbf{u} = \mathbf{x}$, and so for all $\mathbf{u} \in \mathcal{X}$,

$$\begin{aligned} \lambda \cdot (\mathbf{k}_{n_j, :, m}(\mathbf{u}, \mathbf{x}) - \mathbf{k}_{n_j, :, m}(\mathbf{x}, \mathbf{x})) &= \\ \lambda \cdot (\mathbf{k}_{n_j, :, m}(\mathbf{u}, \mathbf{x}) - \mathbf{k}_{n_j, :, m}(\mathbf{x}_{n_j, \lambda}^*, \mathbf{x})) - \lambda \cdot (\mathbf{k}_{n_j, :, m}(\mathbf{x}, \mathbf{x}) - \mathbf{k}_{n_j, :, m}(\mathbf{x}_{n_j, \lambda}^*, \mathbf{x})) &\rightarrow 0 \end{aligned}$$

as $j \rightarrow \infty$ almost surely. By Proposition A.12, $\mathbf{k}_{n, :, m}(\mathbf{u}, \mathbf{x}) - \mathbf{k}_{n, :, m}(\mathbf{u}, \mathbf{x}) \rightarrow \mathbf{k}_{\infty, :, m}(\mathbf{u}, \mathbf{x}) - \mathbf{k}_{\infty, :, m}(\mathbf{u}, \mathbf{x})$ as $n \rightarrow \infty$. We have shown that this limit is zero, since the limit of a subsequence is zero. This is Equation (29).

Hence, for all $\mathbf{u} \in \mathcal{X}$, $\lambda \cdot \mathbf{k}_{\infty, :, m}(\mathbf{u}, \mathbf{x}) = \lambda \cdot \mathbf{k}_{\infty, :, m}(\mathbf{x}, \mathbf{x})$. This also holds for all $\lambda \in \Lambda$ and $m \in \{1, \dots, M\}$, so $\mathbf{K}_\infty(\mathbf{u}, \mathbf{x}) = \mathbf{K}_\infty(\mathbf{x}, \mathbf{x})$. Furthermore, it holds for all $\mathbf{x} \in \mathcal{X}$ and so, using the symmetry of \mathbf{K}_∞ in its arguments, we have,

$$\forall \mathbf{x}, \mathbf{u}, \mathbf{x}', \mathbf{u}' \in \mathcal{X}, \quad \mathbb{P}(\mathbf{K}_\infty(\mathbf{u}, \mathbf{x}) = \mathbf{K}_\infty(\mathbf{u}', \mathbf{x}')) = 1.$$

To extend this to a statement about all choices of $\mathbf{x}, \mathbf{u} \in \mathcal{X}$ simultaneously, observe that \mathcal{X} is a compact metric space and thus is separable. That is, it has a countable, dense subset $\mathcal{X}' \subset \mathcal{X}$. By countable subadditivity of \mathbb{P} , we have

$$\mathbb{P}(\forall \mathbf{x}, \mathbf{u}, \mathbf{x}', \mathbf{u}' \in \mathcal{X}', \quad \mathbf{K}_\infty(\mathbf{u}, \mathbf{x}) = \mathbf{K}_\infty(\mathbf{u}', \mathbf{x}')) = 1.$$

Then, by continuity of the sample paths of \mathbf{K}_∞ , this statement extends to all of \mathcal{X} ,

$$\mathbb{P}(\forall \mathbf{x}, \mathbf{u}, \mathbf{x}', \mathbf{u}' \in \mathcal{X}, \quad \mathbf{K}_\infty(\mathbf{u}, \mathbf{x}) = \mathbf{K}_\infty(\mathbf{u}', \mathbf{x}')) = 1.$$

That is, the sample paths of \mathbf{K}_∞ are almost surely constant. \square

Lemma A.14. *If \mathbf{K}_∞ has almost surely constant sample paths then $\mathbf{f} - \boldsymbol{\mu}_\infty$ has almost surely constant sample paths.*

Proof. Let $\mathbf{u}, \mathbf{x} \in \mathcal{X}$. Then

$$\begin{aligned} \text{Var}_\infty[(\mathbf{f}(\mathbf{u}) - \boldsymbol{\mu}_\infty(\mathbf{u})) - (\mathbf{f}(\mathbf{x}) - \boldsymbol{\mu}_\infty(\mathbf{x}))] &= \\ = \text{Var}_\infty[\mathbf{f}(\mathbf{u}) - \mathbf{f}(\mathbf{x})] &= \underbrace{\mathbf{K}_\infty(\mathbf{u}, \mathbf{u}) - \mathbf{K}_\infty(\mathbf{x}, \mathbf{u})}_{0 \text{ a.s.}} + \underbrace{\mathbf{K}_\infty(\mathbf{x}, \mathbf{x}) - \mathbf{K}_\infty(\mathbf{u}, \mathbf{x})}_{0 \text{ a.s.}} = 0. \end{aligned}$$

Noting that $\mathbb{E}_\infty[(\mathbf{f}(\mathbf{u}) - \boldsymbol{\mu}_\infty(\mathbf{u})) - (\mathbf{f}(\mathbf{x}) - \boldsymbol{\mu}_\infty(\mathbf{x}))] = 0$ almost surely, we can extend this result to the unconditional variance using the law of total variance

$$\begin{aligned} \text{Var}[(\mathbf{f}(\mathbf{u}) - \boldsymbol{\mu}_\infty(\mathbf{u})) - (\mathbf{f}(\mathbf{x}) - \boldsymbol{\mu}_\infty(\mathbf{x}))] &= \\ = \mathbb{E} \left[\underbrace{\text{Var}_\infty[(\mathbf{f}(\mathbf{u}) - \boldsymbol{\mu}_\infty(\mathbf{u})) - (\mathbf{f}(\mathbf{x}) - \boldsymbol{\mu}_\infty(\mathbf{x}))]}_{=0 \text{ a.s.}} \right] &+ \\ + \text{Var} \left[\underbrace{\mathbb{E}_\infty[(\mathbf{f}(\mathbf{u}) - \boldsymbol{\mu}_\infty(\mathbf{u})) - (\mathbf{f}(\mathbf{x}) - \boldsymbol{\mu}_\infty(\mathbf{x}))]}_{=0 \text{ a.s.}} \right] &= \\ = 0. & \end{aligned}$$

Therefore, $(\mathbf{f}(\mathbf{u}) - \boldsymbol{\mu}_\infty(\mathbf{u})) - (\mathbf{f}(\mathbf{x}) - \boldsymbol{\mu}_\infty(\mathbf{x}))$ is a random vector with zero mean and a zero covariance matrix, and so $\mathbf{f}(\mathbf{u}) - \boldsymbol{\mu}_\infty(\mathbf{u}) = \mathbf{f}(\mathbf{x}) - \boldsymbol{\mu}_\infty(\mathbf{x})$ almost surely.

For each pair $\mathbf{x}, \mathbf{u} \in \mathcal{X}$, this holds with probability 1. To conclude that it holds with probability 1 for all $\mathbf{x}, \mathbf{u} \in \mathcal{X}$ simultaneously, we use the same argument as at the end of Lemma A.13. For this, we need only observe that \mathcal{X} is separable and that the sample paths of \mathbf{f} and $\boldsymbol{\mu}_\infty$ are continuous. \square

Having shown that μ_∞ approximates \mathbf{f} up to a constant, we can now strengthen Theorem A.8. This is not necessary for the proof of Theorem A.11, but does improve our understanding of the behaviour of the MOKG.

Corollary A.15. *Suppose we select samples using C-MOKG with random scalarization weights $\lambda_1, \lambda_2, \dots$ chosen independently according to distribution $p(\lambda)$. Then,*

$$\forall \lambda \in \Lambda, \quad \mathbb{P} \left(\sup_{\mathbf{x} \in \mathcal{X}, m \in [M]} \alpha_{\text{C-MOKG}}^n(\mathbf{x}, m; \lambda, \mathbf{c}) \rightarrow 0 \quad \text{as } n \rightarrow \infty \right) = 1.$$

Proof. Let $\lambda \in \Lambda$. By Lévy's zero-one law, $\mathbb{E}_n[\max_{\mathbf{x} \in \mathcal{X}} \lambda \cdot \mathbf{f}(\mathbf{x})] \rightarrow \mathbb{E}_\infty[\max_{\mathbf{x} \in \mathcal{X}} \lambda \cdot \mathbf{f}(\mathbf{x})]$ as $n \rightarrow \infty$ almost surely. Further, we showed in Proposition A.12 that $\mu_n \rightarrow \mu_\infty$ uniformly as $n \rightarrow \infty$ almost surely. Therefore, the residual uncertainty also converges,

$$H_n(\lambda) = \mathbb{E}_n \left[\max_{\mathbf{x} \in \mathcal{X}} \lambda \cdot \mathbf{f}(\mathbf{x}) \right] - \max_{\mathbf{x} \in \mathcal{X}} \lambda \cdot \mu_n(\mathbf{x}) \rightarrow \mathbb{E}_\infty \left[\max_{\mathbf{x} \in \mathcal{X}} \lambda \cdot \mathbf{f}(\mathbf{x}) \right] - \max_{\mathbf{x} \in \mathcal{X}} \lambda \cdot \mu_\infty(\mathbf{x}) = H_\infty(\lambda)$$

as $n \rightarrow \infty$ almost surely. However, from Lemma A.14, the sample paths of $\mathbf{f} - \mu_\infty$ are almost surely constant and so $\max_{\mathbf{x} \in \mathcal{X}} \lambda \cdot \mathbf{f}(\mathbf{x}) = \lambda \cdot \mathbf{f}(\mathbf{x}_{\infty, \lambda}^*)$ almost surely. Hence,

$$H_n(\lambda) \rightarrow H_\infty(\lambda) = \mathbb{E}_\infty[\lambda \cdot \mathbf{f}(\mathbf{x}_{\infty, \lambda}^*)] - \lambda \cdot \mu_\infty(\mathbf{x}_{\infty, \lambda}^*) = 0 \quad (\text{a.s.}).$$

Finally, we note that by Lemma A.5,

$$0 \leq \sup_{\mathbf{x} \in \mathcal{X}, m \in [M]} \alpha_{\text{C-MOKG}}^n(\mathbf{x}, m; \lambda, \mathbf{c}) \leq H_n(\lambda) \rightarrow 0$$

and so $\sup_{\mathbf{x} \in \mathcal{X}, m \in [M]} \alpha_{\text{C-MOKG}}^n(\mathbf{x}, m; \lambda, \mathbf{c}) \rightarrow 0$ as $n \rightarrow \infty$ almost surely. \square

Following Lemma A.14, we can now also prove Theorem A.11.

Proof of Theorem A.11. Let $\lambda \in \Lambda$. Recall that in Equation (27), for each n , we have defined $\mathbf{x}_{n, \lambda}^* \in \arg \max \mathbb{E}_n[\lambda \cdot \mathbf{f}]$ to be a random variable which maximises the posterior mean of the scalarised objective at stage n . Similarly, let $\mathbf{x}_\lambda^* \in \arg \max \lambda \cdot \mathbf{f}$ be a random variable maximizing the scalarised objective $\lambda \cdot \mathbf{f}$. Note that these choices are not necessarily unique.

We wish to first show that $\lambda \cdot \mathbf{f}(\mathbf{x}_{n, \lambda}^*) \rightarrow \lambda \cdot \mathbf{f}(\mathbf{x}_\lambda^*)$ almost surely. By definition of \mathbf{x}_λ^* , the quantity $\lambda \cdot \mathbf{f}(\mathbf{x}_\lambda^*) - \lambda \cdot \mathbf{f}(\mathbf{x}_{n, \lambda}^*)$ is non-negative for each n . Therefore, it suffices to prove that, almost surely, $\limsup_{n \rightarrow \infty} \lambda \cdot \mathbf{f}(\mathbf{x}_\lambda^*) - \lambda \cdot \mathbf{f}(\mathbf{x}_{n, \lambda}^*) \leq 0$.

Observe that we may split the limit superior to give

$$\begin{aligned} & \limsup_{n \rightarrow \infty} \lambda \cdot \mathbf{f}(\mathbf{x}_\lambda^*) - \lambda \cdot \mathbf{f}(\mathbf{x}_{n, \lambda}^*) \\ & \leq \limsup_{n \rightarrow \infty} \left(\lambda \cdot \mathbf{f}(\mathbf{x}_\lambda^*) - \lambda \cdot \mu_\infty(\mathbf{x}_\lambda^*) \right) - \left(\lambda \cdot \mathbf{f}(\mathbf{x}_{n, \lambda}^*) - \lambda \cdot \mu_\infty(\mathbf{x}_{n, \lambda}^*) \right) \\ & \quad + \limsup_{n \rightarrow \infty} \left(\lambda \cdot \mu_\infty(\mathbf{x}_\lambda^*) - \lambda \cdot \mu_n(\mathbf{x}_\lambda^*) \right) - \left(\lambda \cdot \mu_\infty(\mathbf{x}_{n, \lambda}^*) - \lambda \cdot \mu_n(\mathbf{x}_{n, \lambda}^*) \right) \\ & \quad + \limsup_{n \rightarrow \infty} \lambda \cdot \mu_n(\mathbf{x}_\lambda^*) - \lambda \cdot \mu_n(\mathbf{x}_{n, \lambda}^*). \end{aligned}$$

By Lemmas A.13 and A.14, the sample paths of $\lambda \cdot \mathbf{f} - \lambda \cdot \mu_\infty$ are almost surely constant and so the first line above is almost surely zero. The middle line is also almost surely zero since $\mu_n \rightarrow \mu_\infty$ uniformly almost surely by Proposition A.12. Finally, the bottom line is at most zero by definition of the $\mathbf{x}_{n, \lambda}^*$. Therefore

$$\limsup_{n \rightarrow \infty} \lambda \cdot \mathbf{f}(\mathbf{x}_\lambda^*) - \lambda \cdot \mathbf{f}(\mathbf{x}_{n, \lambda}^*) \leq 0$$

as desired and we conclude that $\lambda \cdot \mathbf{f}(\mathbf{x}_{n, \lambda}^*) \rightarrow \lambda \cdot \mathbf{f}(\mathbf{x}_\lambda^*)$ almost surely. \square

B. Further Experimental Details

This section contains further technical details of the experiments described in the main text.

B.1. Test Problems

Two families of test problem are presented, $f^* : [0, 1]^2 \rightarrow \mathbb{R}^2$. They are generated by sampling a GP for each objective. In the first family, the objectives differ in their length scale, while in the second family they differ in the presence of additive, Gaussian observation noise. Table 1 shows the hyper-parameters used for both GPs. Figure 1 in the main text and Figure 5 below show examples of a test problem from the first and second families respectively.

When we sample the GP, we do not know the future locations at which the BO algorithm will try to sample it. To get around this, we sample each GP at 100 points, distributed over $[0, 1]^2$ using a scrambled, 2-dimensional Sobol’ sequence. We then use the posterior mean of the GP after conditioning on these points, as the test function.

Table 1. Hyper-parameters for the Gaussian processes used to generate the two families of test problem.

	FAMILY 1		FAMILY 2	
	OBJECTIVE 1	OBJECTIVE 2	OBJECTIVE 1	OBJECTIVE 2
KERNEL	MATÉRN-5/2	MATÉRN-5/2	MATÉRN-5/2	MATÉRN-5/2
ISOTROPIC LENGTH SCALE	0.2	1.8	0.4	0.4
OUTPUT SCALE	1	50	1	1
CONSTANT MEAN	0	0	0	0
NOISE STANDARD DEVIATION	0	0	1	0

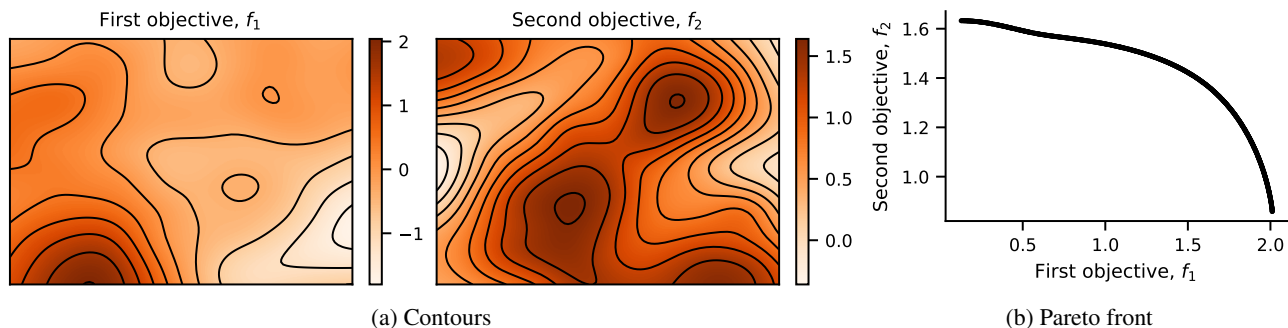


Figure 5. An example from the second set of test problems generated as samples of a GP. Panel (a) shows that both objectives have the same length scale. Instead, the first objective is made harder-to-learn by adding observation noise when sampling. Panel (b) shows the Pareto front of the test problem.

B.2. Surrogate Model

To model the objectives during the Bayesian optimization, we use independent GPs for the objectives. We use a Matérn-5/2 kernel and at each step we fit the hyper-parameters to the data observed so far using maximum a posteriori (MAP) estimates. Before fitting the GP, the observations are standardized to have zero mean and unit variance. This is a common trick used for real-world problems where the prior distributions must be specified based on the data. The reverse transformation is applied when making predictions with the GP.

Prior mean The prior mean of the GP is modelled as a constant function. Bayesian optimization seeks to sample points with large objective values and so fitting the prior mean to this biased sample would introduce a bias to the inferred value. Therefore, the mean was fitted as part of the MAP estimate on the initial six data points, but then held fixed at this value for all future iterations while the other hyper-parameters were fitted.

Observation noise The observation model in Equation (3) contains additive Gaussian observation noise. The variance for this observation noise is only fitted for the first objective in the second family of test problems, since this is the only objective where noise is added. In the first family of test problems and for the second objective of the second family, the variance of the noise was fixed at a negligible value of 10^{-4} . It was not set to zero since this leads to numerical instability. Usually experimenters know whether their problem is stochastic or deterministic, so we view this as the most natural way to model the objectives.

Prior distributions For the length scales, output scales and observation noise variance (where it is fitted), a Gamma prior distribution is used. The Gamma distribution is parameterized by a shape parameter α and a rate parameter β . It is supported on $(0, \infty)$ and has probability density function given by

$$p(z) = \frac{\beta^\alpha}{\Gamma(\alpha)} z^{\alpha-1} e^{-\beta z} \quad (30)$$

where Γ is the gamma function.

The GP prior mean is modelled as a constant function. A uniform distribution across the whole real line is used as an improper prior for this constant. This is implemented by simply not adding any contribution from the prior distribution on the GP prior mean to the marginal log-likelihood.

As explained in the main text, information on which objective has the shorter length scale is included in the prior distributions used for the first family of test problems. Conversely, the priors on the length scales of the objectives in the second problem are identical. Figures 6 and 7 show the prior distributions on the length scales used to model the two families of test problems.

Prior distributions for all the hyper-parameters are summarized in Tables 2 and 3.

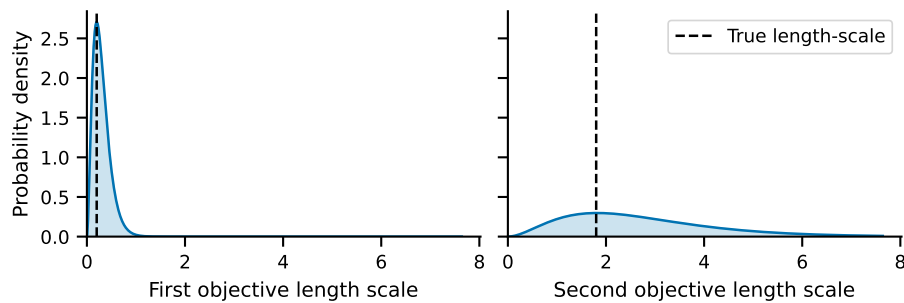


Figure 6. Prior distributions on the length scales for the surrogate model used for the first family of test problems. These encode prior information that the first objective has a shorter length scale.

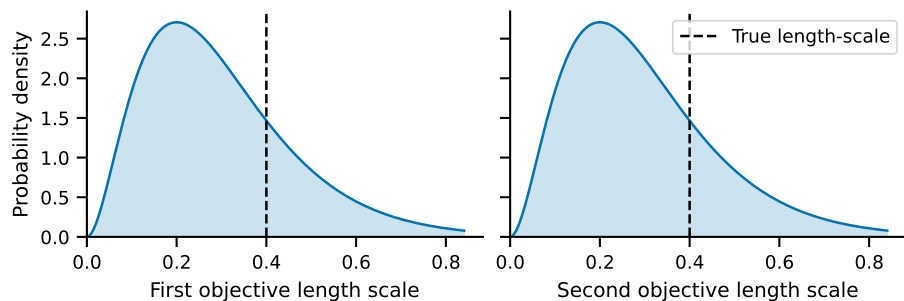


Figure 7. Prior distributions on the length scales for the surrogate model used for the second family of test problems. The same prior is used for both objectives.

Table 2. Prior distributions used for the hyper-parameters of the surrogate model for the standardized data in the first family of test problems.

	OBJECTIVE 1	OBJECTIVE 2
KERNEL	MATÉRN-5/2	MATÉRN-5/2
ISOTROPIC LENGTH SCALE	$\text{Gamma}(\alpha = 3, \beta = 10)$	$\text{Gamma}(\alpha = 3, \beta = 1.1)$
OUTPUT SCALE	$\text{Gamma}(\alpha = 2, \beta = 0.15)$	$\text{Gamma}(\alpha = 2, \beta = 0.15)$
CONSTANT MEAN	NO PRIOR	NO PRIOR
NOISE VARIANCE	FIXED AT 10^{-4}	FIXED AT 10^{-4}

Table 3. Prior distributions used for the hyper-parameters of the surrogate model for the standardized data in the second family of test problems.

	OBJECTIVE 1	OBJECTIVE 2
KERNEL	MATÉRN-5/2	MATÉRN-5/2
ISOTROPIC LENGTH SCALE	$\text{Gamma}(\alpha = 3, \beta = 10)$	$\text{Gamma}(\alpha = 3, \beta = 10)$
OUTPUT SCALE	$\text{Gamma}(\alpha = 2, \beta = 0.15)$	$\text{Gamma}(\alpha = 2, \beta = 0.15)$
CONSTANT MEAN	NO PRIOR	NO PRIOR
NOISE VARIANCE	$\text{Gamma}(\alpha = 1.1, \beta = 0.05)$	FIXED AT 10^{-4}

B.3. Random Numbers

When comparing C-MOKG to the benchmark algorithm, we tried to keep as much as possible the same throughout the experiment. Consequently,

- the algorithms were tested on the same 100 test problems in each family;
- each test problem was assigned a different set of six initial points, which were used for both algorithms;
- the same sequence of points were used in the Monte-Carlo approximations to approximate the expectation over λ in both algorithms.